The COMMUNICATION and
CONTROL SYSTEMS LABORATORY

AD734781

MOMENT METHODS FOR THE IDENTIFICATION
OF THREE DIMENSIONAL
OBJECTS FROM OPTICAL IMAGES

Sahibsingh A. Dudani

August 1971

Department of ELECTRICAL ENGINEERING

DOCUMENT CONTROL DATA - R & D

(Security classification of title, body of abstract and indexing annotation must be entered when the overall report is classified)

1. ORIGINATING ACTIVITY *(Corporate author)*	2a. REPORT SECURITY CLASSIFICATION
Ohio State University Research Foundation Dept of Electrical Engineering Columbus, Ohio 43210	UNCLASSIFIED
	2b. GROUP

3. REPORT TITLE

MOMENT METHODS FOR THE IDENTIFICATION OF THREE DIMENSIONAL OBJECTS FROM OPTICAL IMAGES

4. DESCRIPTIVE NOTES *(Type of report and inclusive dates)*
Scientific   Interim

5. AUTHOR(S) *(First name, middle initial, last name)*

Sahibsingh A.   Dudani

6. REPORT DATE	7a. TOTAL NO. OF PAGES	7b. NO. OF REFS
August 1971	105	29

8a. CONTRACT OR GRANT NO.	9a. ORIGINATOR'S REPORT NUMBER(S)
AFOSR 71-2048	
b. PROJECT NO.	
9769	
c. 61102F	9b. OTHER REPORT NO(S) *(Any other numbers that may be assigned this report)*
d. 681304	AFOSR

10. DISTRIBUTION STATEMENT

Approved for public release;
distribution unlimited.

11. SUPPLEMENTARY NOTES	12. SPONSORING MILITARY ACTIVITY
TECH, OTHER	Air Force Office of Scientific Research 1400 Wilson Blvd Arlington, Va. 22209 (NM)

13. ABSTRACT

The approach presented here makes use of the theory of two-dimensional moment invariants for planar geometric figures developed by Ming-kue Hu [1]. Complete systems of moment invariants under translation, similitude and orthogonal transformations are derived. By carefully utilizing these properties, a sample set is constructed in which each sample is represented by a vector which characterizes the image for a certain orientation of some object from the given group. A pattern recognition technique is then described in which a parametric representation of the input signal is employed. The decision process using typical samples partitions the space into regions that envelop the chosen samples of a class. A simulation program based on the above outline is successfully developed which not only identifies objects, but also determines their orientation and position in space.

DD

MOMENT METHODS FOR THE IDENTIFICATION
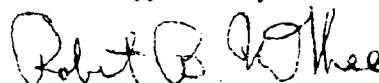OF THREE DIMENSIONAL OBJECTS
FROM OPTICAL IMAGES

A Thesis

Presented in Partial Fulfillment of the Requirements
for the Degree Master of Science

by

Sahibsingh Amulsingh Dudani, B. Tech.

The Ohio State University
1971

Approved by

Adviser
Department of Electrical Engineering

ACKNOWLEDGMENTS

TABLE OF CONTENTS

TABLE OF CONTENTS (Continued)

Chapter

TABLE OF CONTENTS

CHAPTER I

INTRODUCTION

The realization of machine recognition of pictorial data has long been a challenging goal, but has seldom been attempted with anything more complex than alphabetic characters. In this thesis the task of recognition of three dimensional objects from their optical images is considered from the view of identifying and estimating the translation and rotation of the object with respect to a given reference frame.

The approach presented here makes use of the theory of two-dimensional moment invariants for planar geometric figures developed by Ming-kue Hu [1]. Complete systems of moment invariants under translation, similitude and orthogonal transformations are derived. By carefully utilizing these properties, a sample set is constructed in which each sample is represented by a vector which characterizes the image for a certain orientation of some object from the given group. A pattern recognition technique is then described in which a parametric representation of the input signal is employed. The decision process using typical samples partitions the space into regions that envelop the chosen samples of a class. A simulation program based on the above outline is successfully developed which not only identifies objects, but also determines their orientation and position in space.

1

In this research three different objects, a F-4B PHANTOM II, a MIRAGE III C, and a MIG 21 aircraft, were considered. The models of these aircraft of scale 1 : 72 are mathematically represented by a "wire model" structure [2] by considering a finite number of points, called nodes, on the body of the model. These nodes are inter-connected to approximate the curved and planar surfaces on the body of the aircraft by a number of straight lines. A simulation program is used to generate the computational model of the silhouette of the aircraft for any position and orientation in space. Certain invariant properties of these images, as mentioned earlier, are used for the construction of the sample sets. Different amounts of noise were added to the points on the boundary of the simulated image to learn about the performance of this method when using unfocused, hazy or unclear optical images.

Besides the identification of aircraft, this approach can also be used for various other problems. A television camera onboard a docking space craft can take a picture of a docking target and thus after estimating translation and rotation, the docking craft can position itself for automatic docking. In addition, this approach can help in developing a robot eye for use on automatic assembly lines in industries.

A review of different pattern recognition techniques related to this research appears in Chapter II. The problem formulation along with a complete set of invariant moments is presented in Chapter III. In Chapter IV, the computational results including the effect of noise

on parameter estimation are given. Conclusions, a summary of the results, and future research areas are discussed in Chapter V. Finally, Appendix I presents documentation of computer programs at the end of the thesis.

CHAPTER II

SURVEY OF PREVIOUS WORK

2.1 Introduction

Munson [3] describes the pattern recognition process in terms of the following three stages where each is considered as an independent component:

TRANSDUCER → PREPROCESSOR → CLASSIFIER.

However, considering the first step, "it is doubtful if recognition occurs before the eyes are directed toward a (known) object, since otherwise we would not bother to look at the object" [4]. Thus it would seem reasonable to use the raw data in the form of the image as bulk memory and allow the transducer to search for "regions of interest" [5]. In considering the three stages, the literature overwhelmingly concentrates on the various aspects of classification. It is here that a substantial objection can be raised. Is not the more significant part of the problem that of characterizing the world by a set of properties that provide the desired discrimination? In fact Selfridge [6] defines pattern recognition solely in terms of "the extraction of significant features from a background of irrelevant detail."

Kazmierczak and Steinbuch [7] state that "the human visual system

is capable of selecting features or criteria from a pattern where the statement of the description would be independent of registration, skew, size, contrast, deformation, or other noise effects." What is needed according to Duda [8] are "rugged features". "A rugged feature is one whose presence is not changed, and whose characteristics are not greatly altered, by normal variations in the image of a character in a given category." It is emphasized, and this is an important point, that no general theory exists to allow us to choose what features are relevant for a particular problem. With these comments in mind, the object of the rest of the chapter is to present a discussion of a few computer methods and algorithms used in conjunction with image analysis.

2.2 Contour Tracing

One of the approaches to reduce the amount of data in a picture involves scanning a picture and tracing a contour or outline of the figure and then basing the recognition or classification decision on this information [9]. It is well known [10], that "contours carry a significant fraction of the information required for recognition of image objects." Examples of this approach applied to character recognition are discussed in the literature [11] - [13].

Hemami, McGhee and Gardner [14] in their paper presented an algorithm which uses the information contained in the boundary of the pattern by successively reading the coordinates of the boundary and developing a nonlinear regression analysis technique for simultaneous estimation of rotation and translation of the image objects. One of

the advantages of using a contour description is that the latter is independent of shape, translation, size and rotation [15].

2.3 Conic Section Approximation

Here we consider shape description in terms of conic sections. An individual pattern is defined as a non-negative function, f, on the real plane, subject to certain constraints on position, size, orientation, etc. In a given frame of reference any conic section may be uniquely represented as

$$Q(x,y) = ax^2 + 2hxy + by^2 + 2gx + 2fy + c = 0, \qquad (2\text{-}1)$$

where $a^2 + 4h^2 + b^2 + 4g^2 + 4f^2 + c = 1$ and the first non zero element of the vector (a, 2h, b, 2g, 2f, c) is positive. Such a vector will be referred to as a conic vector.

The true Euclidian distance from a point (u,v) to the nearest point on the conic Q(x,y) = 0 is a troublesome quantity to evaluate, and we use instead the quantity $|Q(uv)|$, which vanishes on and only on the conic and, loosely speaking, takes larger values for points (u,v) further from the conic. The weighted squared discrepancy between the pattern, P, and the conic may then be defined as

$$D = \iint P(u,v) \ |Q(uv)|^2 \ du \ dv, \qquad (2\text{-}2)$$

and the "best" conic is that for which D is the least. This problem may be formulated as an eigen value problem of order six, the conic

vector corresponding to the smallest root defining the best conic [16].

The best conic approximation has been used by Paton [16] as a discriminator in chromosome analysis. An example of a best conic approximation to a certain chromosome pattern is shown in Fig. 2.1.
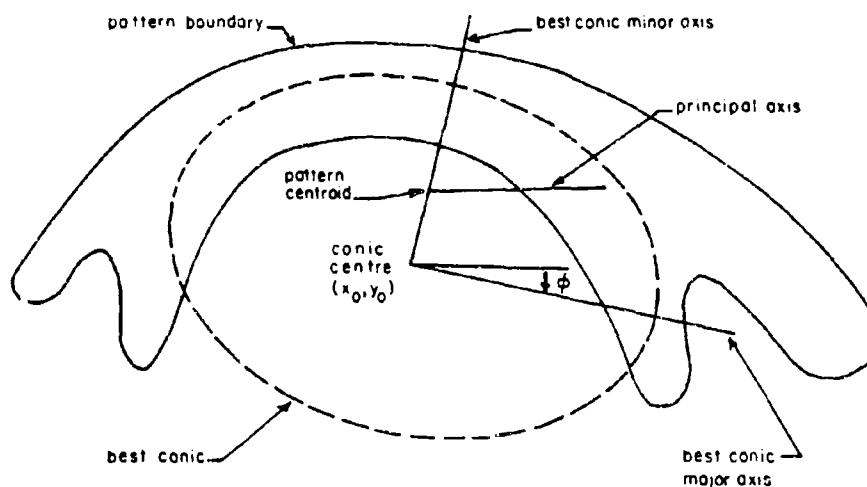
Figure 2.1 Line Drawing of a Chromosome Pattern and its Best Conic Approximation

2.4 Shape Descriptors

Intuitively, it is preferable to describe an object using gross

properties rather than local or neighborhood descriptors. Shape description is undoubtedly one of the most important aspects of pattern recognition. It is desirable in many applications to describe the structure of an object independently of orientation, translation or even some types of distortion. Interesting discussions regarding recognition of shape and their computer models can be found in papers of Blum [17], [18].

Based on some shape description theories, an interesting shape descriptor referred to as a medial axis transformation (MAT) was developed by Blum [18]. He describes the generating model which is used to define MAT: " Consider a continuous isotropic plane that has the following properties at each point: 1) excitation – each point can have a value of 0 or 1, 2) propagation – each excited point excites an adjacent point with a delay proportional to the distance, and 3) refractory or dead time – once fixed, an excited point is not affected by a second firing for some arbitrary interval of time. A visual stimulus from which the contours or edges have been extracted impinges on such a plane at some fixed time and excites the plane at those points. This excitation spreads uniformly in all directions but in such a way that the waves generated do not flow through each point."

The MAT is then defined as the locus of the corners in the wavefront. The (propagating) contours have been likened to the front of a grassfire ignited on the pattern boundary and the MAT is then the locus of points where the fire is extinguished. Several examples of MATs are shown in Fig. 2.2. Note that, if the MAT turns out to be a
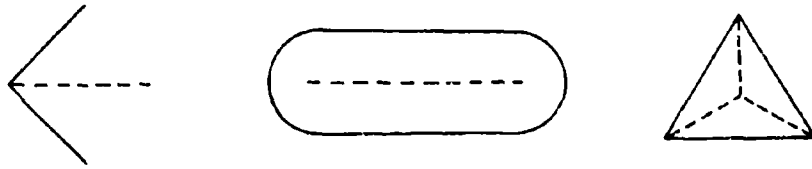
Figure 2.2   Examples of MAT Transformation
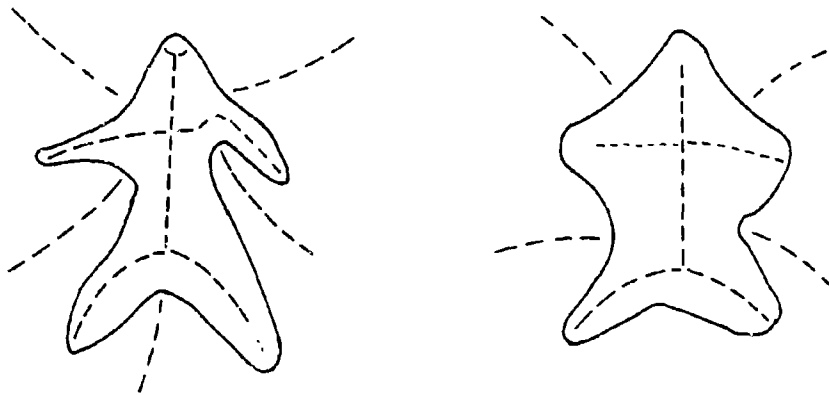
Figure 2.3   The MAT for Both a Simple Sketch
and a Distorted Version of a Man

straight line, then the shape of the object under consideration is symmetrical. The gross properties of the transformation are obviously related to the macroscopic and structural properties of the pattern. This is demonstrated by Blum [18] using both a sketch-like representation of a human and its distorted version as shown in Figure 2.3. The basic properties of the MAT remain unchanged.

2.5 Moment Transformations

A set of two-dimensional moment invariants have been found by Hu [1]. Based upon these moment invariants, a pattern-recognition theory has been formulated which considers two patterns to be similar if they differ at most in the following respects:

(A) Location

(B) Size

(C) Orientation

With the help of moment transformations, we can find a pattern function as a number $m = F(P)$ associated with each pattern, P, which is

(a) invariant under (A) to (C), i.e., if patterns P_1 and P_2 are similar according to (A) to (C) then $F(P_1) = F(P_2)$;

(b) characteristic of dissimilar patterns, i.e., if patterns P_1 and P_2 are not similar according to (A) to (C) then $F(P_1) \neq F(P_2)$;

(c) easy to compute.

If such a function cannot be found, then one might try to use several functions $F_1(P)$, $F_2(P)$, ..., which satisfy (a) and (c), though not (b), in the hope that for any given pair P_1 and P_2 of dissimilar patterns, at least one of the functions $F_i(P)$ would give $F_i(P_1) \neq F_i(P_2)$.

The latter is the approach we propose to follow.

2.5.1 Definition of Two Dimensional Moments

Let there be N points equally distributed along the boundary of a certain pattern as shown in Figure 2.4.
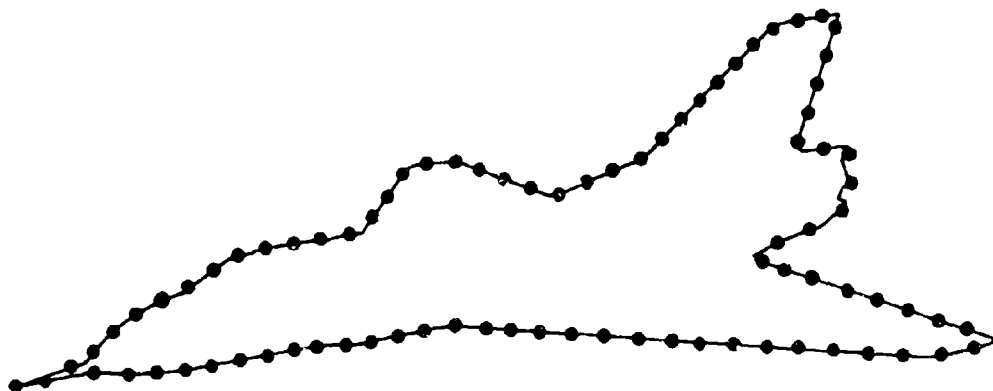
Figure 2.4 Discrete Representation of the Boundary of a Pattern

Let the coordinates of these points be (x_1,y_1), (x_2,y_2), ..., (x_N,y_N). Then the two dimensional $(p+q)^{th}$ order moments are defined as

$$m_{pq} = \frac{1}{N} \sum_{i=1}^{N} x_i^{p} y_i^{q} \ , \quad p + q = 0,1,2, \ldots \ . \tag{2-3}$$

Also let $(\bar{x}, \bar{y})$ be the centroid of the given pattern. Then,

$$N \cdot \bar{x} = \sum_{i=1}^{N} x_i$$

or

$$\bar{x} = \frac{1}{N} \sum_{i=1}^{N} x_i = m_{10} \quad . \tag{2-4}$$

Similarly

$$\bar{y} = m_{01} \quad . \tag{2-5}$$

2.5.2 Central Moments

The central moments are defined as

$$u_{pq} = \frac{1}{N} \sum_{i=1}^{N} (x - \bar{x})^p (y - \bar{y})^q \tag{2-6}$$

where

$$\bar{x} = m_{10} \quad , \quad \bar{y} = m_{01} \quad . \tag{2-7}$$

It should be noted that $u_{01} = u_{10} = 0$. Now, let us consider the effect of translation on these central moments. Let

$$x_i' = x_i + \alpha \tag{2-8}$$

$$y_i' = y_i + \beta \tag{2-9}$$

where α, β are constants. Then,

$$m_{10}' = \frac{1}{N} \sum_{i=1}^{N} x_i'$$

$$= \frac{1}{N} \sum_{i=1}^{N} x_i + \frac{N \cdot \alpha}{N}$$

$$= m_{10} + \alpha \qquad (2-10)$$

or

$$\overline{x}' = \overline{x} + \alpha . \qquad (2-11)$$

Similarly

$$\overline{y}' = \overline{y} + \beta . \qquad (2-12)$$

Using this new centroid of the pattern, let us now calculate the new central moments under translation.

$$u_{pq}' = \frac{1}{N} \sum_{i=1}^{N} (x_i' - \overline{x}')^p (y_i' - \overline{y}')^q$$

$$= \frac{1}{N} \sum_{i=1}^{N} (x_i + \alpha - \overline{x} - \alpha)^p (y_i + \beta - \overline{y} - \beta)^q$$

$$= u_{pq} \qquad (2-13)$$

Thus the central moments are invariant under translation.

From Eq. (2-6) it is quite easy to express central moments in terms of ordinary moments. For the first three orders,

$$u_{00} = m_{00} = 1 \tag{2-14}$$

$$u_{01} = u_{10} = 0 \tag{2-15}$$

$$u_{20} = m_{20} - (m_{10})^2 \tag{2-16}$$

$$u_{02} = m_{02} - (m_{01})^2 \tag{2-17}$$

$$u_{30} = m_{30} - 3m_{20}m_{10} + 2(m_{10})^3 \tag{2-18}$$

$$u_{21} = m_{21} - m_{20}m_{01} - 2m_{11}m_{10} + 2(m_{10})^2 m_{01} \tag{2-19}$$

$$u_{12} = m_{12} - m_{02}m_{10} - 2m_{11}m_{01} + 2(m_{01})^2 m_{10} \tag{2-20}$$

$$u_{03} = m_{03} - 2m_{11}m_{01} + 2(m_{01})^2 \tag{2-21}$$

From here on, for simplicity of description, all moments referred to are central moments and u_{pq} will be simply expressed as:

$$u_{pq} = \frac{1}{N} \sum_{i=1}^{N} x_i{}^p y_i{}^q \quad . \tag{2-22}$$

2.5.3 Similitude Moment Invariants

Under a similitude transformation, i.e., change of size, we have

$$\begin{bmatrix} x' \\ y' \end{bmatrix} = \begin{bmatrix} \gamma & 0 \\ 0 & \gamma \end{bmatrix} \begin{bmatrix} x \\ y \end{bmatrix} , \gamma = \text{constant} \quad (2\text{-}23)$$

Let us now calculate the new central moments u'_{pq} after the transformation.

$$u'_{pq} = \frac{1}{N} \sum_{i=1}^{N} x_i'^{p} \, y_i'^{q} \quad (2\text{-}24)$$

$$= \frac{1}{N} \sum_{i=1}^{N} \gamma^{p} x_i^{p} \, \gamma^{q} y_i^{q}$$

$$= \gamma^{p+q} \, \frac{1}{N} \sum_{i=1}^{N} x_i^{p} \, y_i^{q}$$

or

$$u'_{pq} = \gamma^{p+q} \, u_{pq} \quad (2\text{-}25)$$

Therefore we have the following absolute similitude moment invariants:

$$\frac{u'_{pq}}{\gamma^{p+q}} = u_{pq} , \quad p + q = 2, 3, \ldots \quad (2\text{-}26)$$

Using similitude invariants of central moments, pattern identification can easily be accomplished independently of translation and size.

2.5.4 Orientation Moment Invariants

Under the orthogonal transformation of rotation,

$$x' = x \cos \theta - y \sin \theta , \qquad (2-27)$$

$$y' = x \sin \theta + y \cos \theta . \qquad (2-28)$$

Thus, the new moments under rotation will be as follows:

$$u_{pq}' = \frac{1}{N} \sum_{i=1}^{N} x'^{p} y'^{q}$$

$$= \frac{1}{N} \sum_{i=1}^{N} (x\cos\theta - y\sin\theta)^{p} (x\sin\theta + y\cos\theta)^{q} \qquad (2-29)$$

$$u_{pq} = \frac{1}{N} \sum_{i=1}^{N} x^{p} y^{q} \qquad (2-30)$$

It can be shown [1] that the three second order moments satisfy the following relations:

$$2u_{11}' = (u_{20} - u_{02}) \sin 2\theta + 2u_{11}\cos 2\theta , \qquad (2-31)$$

$$u_{20}' + u_{02}' = u_{20} + u_{02} , \qquad (2-32)$$

$$(u_{20}' - u_{02}')^2 + 4(u_{11}')^2 = (u_{20} - u_{02})^2 + 4u_{11}^2 . \quad (2\text{-}33)$$

There are two ways of using Eqs. (2-31), (2-32) and (2-33) to accomplish pattern identification independently of orientation:

(A) The method of principal axes: if the angle θ is determined from the equation (2-31) to make $u_{11}' = 0$, then we have,

$$\tan 2\theta = -2u_{11}/(u_{20} - u_{02}). \quad (2\text{-}34)$$

The x', y' axes determined by any particular value of θ satisfying Eq. (2-34) are called principal axes of the pattern. With added restriction, such as $u_{20}' > u_{02}'$ and $u_{30}' > 0$, θ can be determined uniquely. Moments determined with respect to such a pair of principal axes are independent of orientation.

(B) The method of orthogonal moment invariants: the two relations Eqs. (2-32) and (2-33) are invariant under rotation, and they can be used directly for orientation-independent pattern identification. Let these two invariant relations be called M_1 and M_2 respectively. The discrimination property can also be increased by including higher-order moment invariants. For third-order moments, we can show that the following four expressions are invariant under orthogonal transformation.

$$M_3 = (u_{30} - 3u_{12})^2 + (3u_{21} - u_{03})^2 \quad (2\text{-}35)$$

$$M_4 = (u_{30} + u_{12})^2 + (u_{21} + u_{03})^2 \qquad (2-36)$$

$$M_5 = (u_{30} - 3u_{12})(u_{30} + u_{12})[(u_{30} + u_{12})^2 - 3(u_{21} + u_{03})^2]$$

$$+ (3u_{21} - u_{03})(u_{21} + u_{03}) \cdot [3(u_{30} + u_{12})^2 - (u_{21} + u_{03})^2] \qquad (2-37)$$

$$M_6 = (u_{20} - u_{02})[(u_{30} + u_{12})^2 - (u_{21} + u_{03})^2]$$

$$+ 4u_{11}(u_{30} + u_{12})(u_{21} + u_{03}) \qquad (2-38)$$

Similarly, higher-order orthogonal moment invariants can be derived. In fact, it has been found that there exists a complete system of infinitely many such invariants [1].

It is interesting to note that in the above methods, because of complete orientation independence property, different patterns which could be obtained from each other by just proper rotation, such as '6' or '9' can not be distinguished. If the given pattern is of circular or n-fold rotational symmetry, then the determination of θ by Eq. (2-34) breaks down. This is due to the fact that both numerator and denominator are zero for such patterns.

2.6 Sample Set Construction and Linear Separatibility

Based on the features extracted from the optical image or the pattern, one can form a sample set which characterizes classes from a small number of their members. In addition to this, pattern recognition techniques must perform a basic function of recognizing a new input

stimulus and classify it as a member of one of several classes.
Machine learning, the automatic accomplishment of classification, re-
quires partitioning the vector space into regions so that each region
should contain mostly members of a single class. The regions so con-
structed characterize the classes. The block diagram shown in Figure
2.5 illustrates a general pattern recognition system that exhibits the
functions discussed above [19]. The parameter extractor is used to
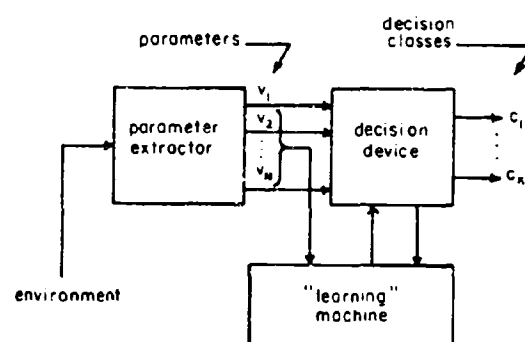
Figure 2.5 General Pattern Recognition System

represent the machine's environment as a vector in an N-dimensional
vector space. Machine learning is employed to determine, from
sample inputs, the best method of partitioning the space into differ-
ent decision regions, and the decision device, which implements the
regions designed through machine learning, evaluates new input stimuli
and classifies them according to the region in which they are con-
tained.

Most of the machines used are linear, employing only linear

discriminants, i.e., correlations with stored reference vectors or comparisons of weighted combinations of the parameters. Hyper-planes are used to partition the space of measurable input parameters to separate members of one stimulus class from those of another. Combinations of these linear techniques with logical rules, can construct boundaries to quite complex distributions. In many practical problems the classes are not linearly separable (not separable by hyperplanes) and their members are not contained in disjointed simply-connected regions of space of observable parameters. In these cases, better decision rules than those provided by linear discriminants should be used to minimize the probability of decision errors [19]. This is illustrated in Figure 2.6 where members of different classes are contained in regions labeled A and B. These classes are linearly separable in Figure 2.6a but not in the more complex distribution shown in Figure 2.6b.
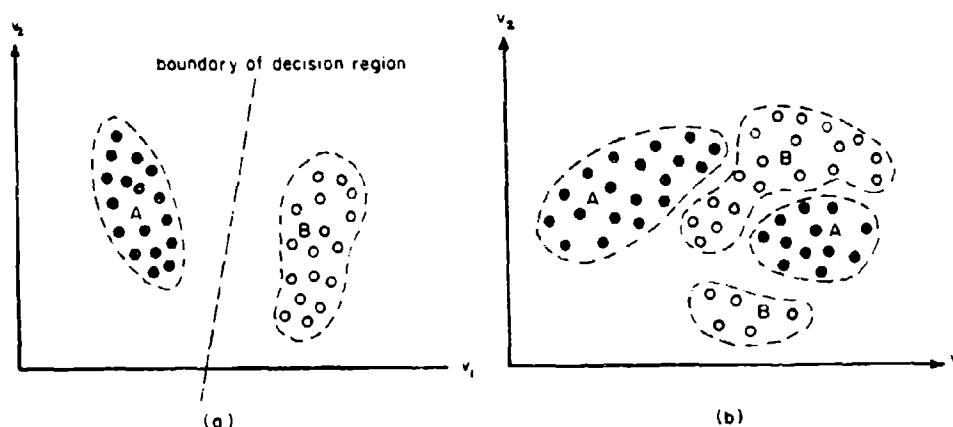
Figure 2.6 Different Distributions of Two Classes

2.7 Recognition of Three-Dimensional Objects

The schemes developed by many authors for the recognition of a solid object from its optical image require the perspective transformation of a three-dimensional field, with hidden lines removed. The perspective projection is used to fit the given picture. The computer oriented techniques of forming perspective projection of a given object are presented by Weiss [20], Comba [21] and Loutrel [22].

Guzman [23] and Winston [24] in their work in the field of recognition of three dimensional objects developed a scheme which recognizes the objects irrespective of their translations and rotations. They consider a three-dimensional structure composed of bricks, wedges and other simple objects. It is assumed in their work that a preprocessing of some sort has taken place, and the picture to be analyzed is available in a symbolic format of points, lines and surfaces. The recognition scheme identifies the object from its picture by selecting a combination of surfaces and relating it to an object.

The only two pattern recognition schemes in the literature, to the author's knowledge, which deal with the estimation of three translations and three rotations associated with the object, are developed by Roberts [25] and Advani [26]. Roberts [25] in his work assumes that the objects seen could be constructed out of some familiar parts, called the models. The procedure starts by first converting the picture into a line diagram; then the points in the line diagram which fit a transformation of some model are found. This model has a set of topological equivalent points. Finally the mean-square error

minimization technique with some threshold is used to eliminate models

which fit the picture topologically, but do not fit exactly without

being deformed. This scheme does not yield the depth information but

relies on a support theorem for the purpose of estimating the depth

or the translation along the optical axis of the camera. This theorem

requires the object in the scene to be supported by the ground or

another object resting on the ground. This is one of the disadvantages

in Roberts' recognition algorithm.

Advani [26] developed an algorithm to estimate the three trans-

lations and three rotations of an object from its silhouette by the

use of regression analysis. Advani, in his work, synthesizes the sil-

houette for a certain translation and rotation, and then tries to

match this synthesized silhouette with the given silhouette of the

object with unknown translation and rotation. Advani's method is

fairly accurate, even in the presence of large amounts of noise, but

the main drawback of this algorithm is that it takes a much longer time

for recognition than what would be needed in many practical appli-

cations. A new technique for recognition of three dimensional objects

is developed in this research which has the potential of reaching real

time identification.

CHAPTER III

PROBLEM FORMULATION

3.1 Introduction

The problem which concerns us may be stated as follows: a digital computer receives an optical image of a three-dimensional object, and on the basis of this information it has to identify the object and estimate its position and orientation in space.

It is assumed here that it is possible to obtain the silhouette of the picture through some type of preprocessing of the optical image [5]. On this silhouette a number of equally spaced data points are generated and used for the calculation of moments. Using these moments, as mentioned earlier, the computer should assign the image to a certain object, and estimate the six parameters to be defined later in section 3.4.

3.2 Transformation of the Real World

The first assumption here is that the picture is a view of the real world recorded by a camera or other comparable device and therefore that the image is a perspective transformation of a three-dimensional field. This transformation is a projection of each point in the viewing space, toward a focal point, onto a plane. The transformation depends on the camera used, the enlargement printing process,

23

and, of course, the coordinate system the real world is referred to.
Let us fix the real world coordinates X, Y and Z by assuming that the
focal plane is the Y = -2f plane, that the focal point is at X = 0,
Y = -f, Z = 0, and the optical axis is colinear with the Y axis. In
order that the picture not be a reflection, we choose the focal plane
in front of the camera. Thus the focal plane is really the plane of
the print, not of the negative. Let U and V represent the coordinates
on the focal plane of the projections for the points in the real
world. This arrangement is shown in Figure 3.1.
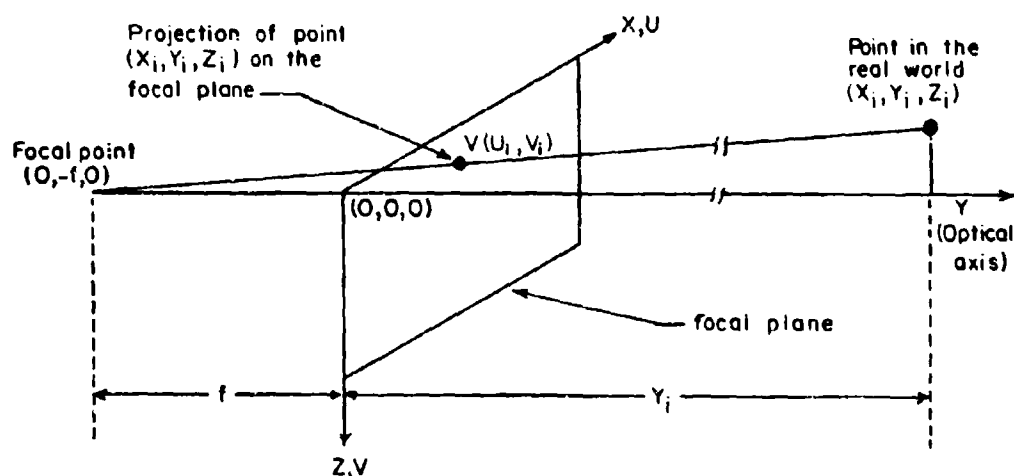
Figure 3.1 Camera Transformation

Let (X_i, Y_i, Z_i) be a point in the viewing space and (U_i, V_i)
be its projection on the focal plane as shown in Figure 3.1 This

transformation is shown below:

$$U_i = \frac{f}{Y_i + f} \cdot X_i \quad , \qquad \text{(3-1)}$$

$$V_i = \frac{f}{Y_i + f} \cdot Z_i \qquad \text{(3-2)}$$

where, f, is the focal length of the camera.

3.3 Mathematical Representation of Three-Dimensional Objects with the Wire Frame Structure

The mathematical representation of the three-dimensional object is achieved by selecting a number of points, depending on the complexity of the structure, on the body of the prototype model of a given scale. These points are referred to as nodes. These nodes are then appropriately interconnected to approximate the planar and curved surfaces on the body of the object by a number of straight lines. This results in a so called "wire-frame" structure [2], because the straight lines could be considered as wires connected between the fixed points (nodes) which form the frame. The connections between different nodes can be mathematically expressed by a connection matrix in which each row represents a certain node, and therefore the connection matrix has the same number of rows as the nodes selected to construct the wire-frame structure. The different column entries for each row in the matrix show the nodes connected to the one represented by the row. The trailing zeroes in a row show that no more nodes are connected to the

node represented by the row. One such example appears in Figure 3.2.

It is to be noted here that the nth row of the connection matrix,

represents the nth node of the object, shown in Figure 3.2.
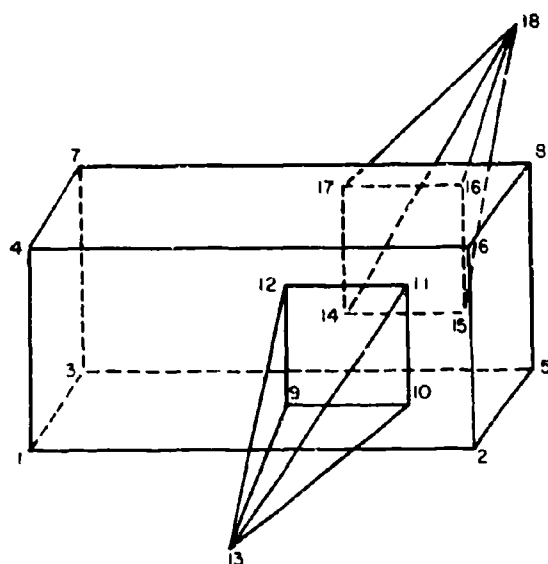
Connection Matrix:

$$
\begin{bmatrix}
2 & 3 & 4 & 0 \\
1 & 5 & 6 & 0 \\
1 & 5 & 7 & 0 \\
1 & 6 & 7 & 0 \\
2 & 3 & 8 & 0 \\
2 & 4 & 8 & 0 \\
3 & 4 & 8 & 0 \\
5 & 6 & 7 & 0 \\
10 & 12 & 13 & 0 \\
9 & 11 & 13 & 0 \\
10 & 12 & 13 & 0 \\
9 & 11 & 13 & 0 \\
9 & 10 & 11 & 12 \\
15 & 17 & 18 & 0 \\
14 & 16 & 18 & 0 \\
15 & 17 & 18 & 0 \\
14 & 16 & 18 & 0 \\
14 & 15 & 16 & 17
\end{bmatrix}
$$

Figure 3.2 Wire Frame Structure and Connection Matrix
for a Winged Parallelepiped

3.4 Transformation Matrix

Let us fix a new coordinate system, xyz, to the center of gravity

of the object to be identified. The coordinates of the nodes, selected

on the body of the prototype of the object for the wire frame structure representation, are measured with respect to this xyz coordinate system. Let the M nodes, selected for a certain object to be identified, have the coordinates $[(x_i, y_i, z_i), i = 1, 2, ..., M]$. At first, let the three axes x, y and z of the coordinate system fixed to the object be colinear with the respective axes, X, Y and Z of the real world coordinates. This is shown by the transformation given below in Eq. (3-3), which relates the coordinates x_i, y_i and z_i of a node to the real world coordinates X_i, Y_i and Z_i.

$$\begin{bmatrix} X_i \\ Y_i \\ Z_i \end{bmatrix} = \begin{bmatrix} x_i \\ y_i \\ z_i \end{bmatrix} \quad i = 1,2, ..., M. \quad (3-3)$$

The relative orientation of two arbitrary orthogonal systems can be specified by a set of no fewer than three angles, usually called Euler angles. Although the concept of the Euler angles is universally used in several applications, there is no agreement on the definition of the Euler angles. There are a large number of possible choices for the three angles required to define an Euler set of angles [27]. A particular set of Euler angles is selected here with the aim of obtaining moment invariance with one of the angles of the set. The transformations for the set of Euler angles selected are shown in Figures 3.3 through 3.6. The symbolic representation used in these figures to accomplish coordinate transformations is straightforward and is

discussed in [28]. The three Euler angles θ, ψ and ϕ are called the elevation, azimuth and roll angles respectively.
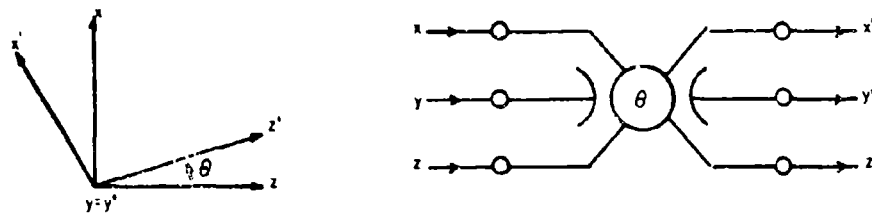
$$x' = -z \sin \theta + x \cos \theta$$

$$y' = y$$

$$z' = z \cos \theta + x \sin \theta$$

Figure 3.3   Elevation Angle Transformation
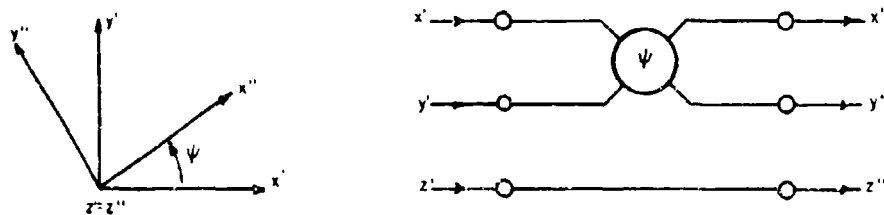
$$x'' = x' \cos \psi + y' \sin \psi$$

$$y'' = -x' \sin \psi + y' \cos \psi$$

$$z'' = z'$$

Figure 3.4   Azimuth Angle Transformation
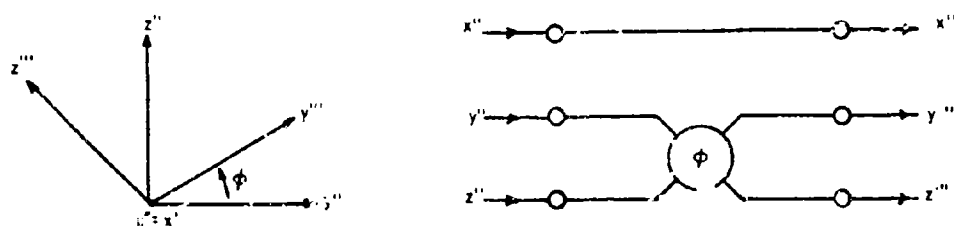
$$x''' = x''$$

$$y''' = y'' \cos \phi + z'' \sin \phi$$

$$z''' = -y'' \sin \phi + z'' \cos \phi$$

Figure 3.5 Roll Angle Transformation
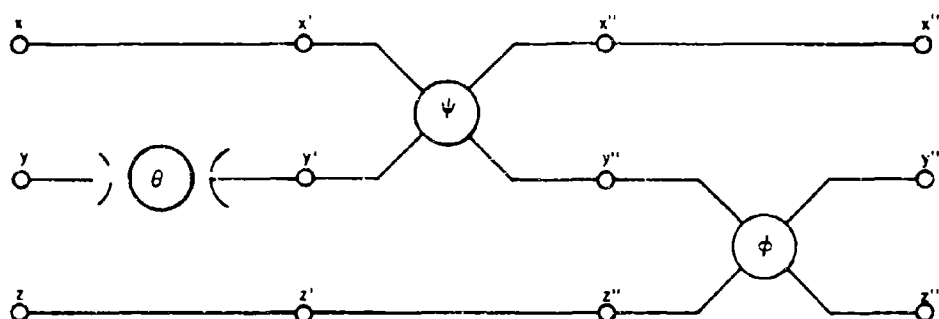
Figure 3.6 Symbolic Representation of the Euler Angle Sequence

The transformation matrix, which relates the coordinates of a node with respect to the two different systems defined earlier, is

as shown below:

$$\begin{bmatrix} X_i \\ Y_i \\ Z_i \end{bmatrix} = \begin{bmatrix} \cos\theta & 0 & \sin\theta \\ 0 & 1 & 0 \\ -\sin\theta & 0 & \cos\theta \end{bmatrix} \begin{bmatrix} \cos\psi & -\sin\psi & 0 \\ \sin\psi & \cos\psi & 0 \\ 0 & 0 & 1 \end{bmatrix} \begin{bmatrix} 1 & 0 & 0 \\ 0 & \cos\phi & -\sin\phi \\ 0 & \sin\phi & \cos\phi \end{bmatrix} \begin{bmatrix} x_i \\ y_i \\ z_i \end{bmatrix}$$

$$\text{for } i = 1, 2, \ldots, M \qquad (3\text{-}4)$$

After giving the above orientation to the xyz system, let us translate the origin of this system to a point (A, B, C) with respect to the real world coordinate system. The modified transformation is given below:

$$\begin{bmatrix} X_i \\ Y_i \\ Z_i \end{bmatrix} = \begin{bmatrix} \cos\theta\cos\psi & -\cos\theta\sin\psi\cos\phi + \sin\theta\sin\phi & \cos\theta\sin\psi\sin\phi + \sin\theta\cos\phi \\ \sin\psi & \cos\psi\cos\phi & -\cos\psi\sin\phi \\ -\sin\theta\cos\psi & \sin\theta\sin\psi\cos\phi + \cos\theta\sin\phi & -\sin\theta\sin\psi\sin\phi + \cos\theta\cos\phi \end{bmatrix} \begin{bmatrix} x_i \\ y_i \\ z_i \end{bmatrix} + \begin{bmatrix} A \\ B \\ C \end{bmatrix}$$

$$\text{for } i = 1, 2, \ldots, M \qquad (3\text{-}5)$$

With the use of this transformation matrix, each node of the wire frame structure can be represented in the XYZ coordinate system, given the three translational and the three rotational parameters. The projection of these M nodes can be obtained on the image plane and used to construct the computational model of the silhouette [26]. This method of simulating the silhouette for a given set of six parameters is used later for the sample set construction.

3.5 Moment Invariance with Angle of Elevation

It will be shown here that the silhouettes obtained for different values of the elevation angle, with the other parameters remaining the same, are similar in size and shape but differ only in rotation. Therefore the moment invariant functions derived in section 2.5.4 characterize this silhouette for the other given parameters.

It will be assumed that the optical axis of the camera is directed to pass through the center of gravity of the object to be identified, and thus the parameters A and C, defined earlier, will take smaller values compared to the distance of the object along the optical axis. This can be accomplished by using some kind of feedback system which will change the direction of the optical axis so as to bring the centroid of the silhouette to the origin of the UV coordinate system.

The projection of a certain point in the viewing space onto the focal plane is given by the following transformation

$$U_i = \frac{f}{f + Y_i} \cdot X_i \quad , \tag{3-6}$$

$$V_i = \frac{f}{f + Y_i} \cdot Z_i \quad , \tag{3-7}$$

where (U_i, V_i) are the coordinates of the projected point in the focal plane. With the assumption that the parameters A and C are small in Eq. (3-5), we have the following relations:

$$Y_i = (\sin\psi)x_i + (\cos\psi \cos\phi)y_i + (-\cos\psi \sin\phi)z_i + B \qquad (3-8)$$

$$X_i = \cos\theta(\cos\psi)x_i + (-\cos\theta \sin\psi \cos\phi + \sin\theta \sin\phi)y_i$$
$$+ (\cos\theta \sin\psi \sin\phi + \sin\theta \cos\phi)z_i \qquad (3-9)$$

$$Z_i = -\sin\theta(\cos\psi)x_i + (\sin\theta \sin\psi \cos\phi + \cos\theta \sin\phi)y_i$$
$$+ (-\sin\theta \sin\psi \sin\phi + \cos\theta \cos\phi)z_i \qquad (3-10)$$

It is interesting to note here that Y_i is not a function of the elevation angle θ and hence remains the same for all values of θ, given the parameters ψ, ϕ and B. Thus the factor $K = f/(f + Y_i)$ in Eqs. (3-6) and (3-7) remains constant with θ, for the given values of ψ, ϕ and B. Therefore we have

$$U_i = K X_i \quad , \qquad (3-11)$$

$$V_i = K Y_i \quad , \qquad (3-12)$$

where K is a constant. It can further be shown that the expression $(X_i^2 + Z_i^2)$ is also not a function of the elevation angle θ, given the assumption $A = C = 0$. Using Eqs. (3-9) and (3-10), we have

$$X_i^2 + Z_i^2 = \cos^2\psi \, x_i^2 + (\sin^2\psi \cos^2\phi + \sin^2\phi)y_i^2$$
$$+ (\cos^2\phi + \sin^2\psi \sin^2\phi)z_i^2 \qquad (3-13)$$

Therefore, using this result along with Eqs. (3-11) and (3-12), we have

$$U_1{}^2 + V_1{}^2 = K^2 (X_1{}^2 + Z_1)^2$$

$$= f(\psi, \phi, B) \qquad (3\text{-}14)$$

This shows that when the elevation angle of a certain object is changed, the locus of the projection of each node of the object onto the focal plane is a circle with the center as the origin. Thus we can in effect say that the result of varying the elevation angle of a certain object, on its silhouette, is just its rotation in the focal plane, with no change in size and shape. Perspective projections with different elevation angles, but with the same azimuth angle, roll angle and distance along optical axis, appear in Figure 3.7. The moment functions M_1, M_2, M_3, M_4, M_5 and M_6 derived earlier in section 2.5.4 are therefore invariant with the elevation angle θ.

$$M_1 = u_{20} + u_{02} \qquad (3\text{-}15)$$

$$M_2 = (u_{20} - u_{02})^2 + 4u_{11}{}^2 \qquad (3\text{-}16)$$

$$M_3 = (u_{30} - 3u_{12})^2 + (3u_{21} - u_{03})^2 \qquad (3\text{-}17)$$

$$M_4 = (u_{30} + u_{12})^2 + (u_{21} + u_{03})^2 \qquad (3\text{-}18)$$
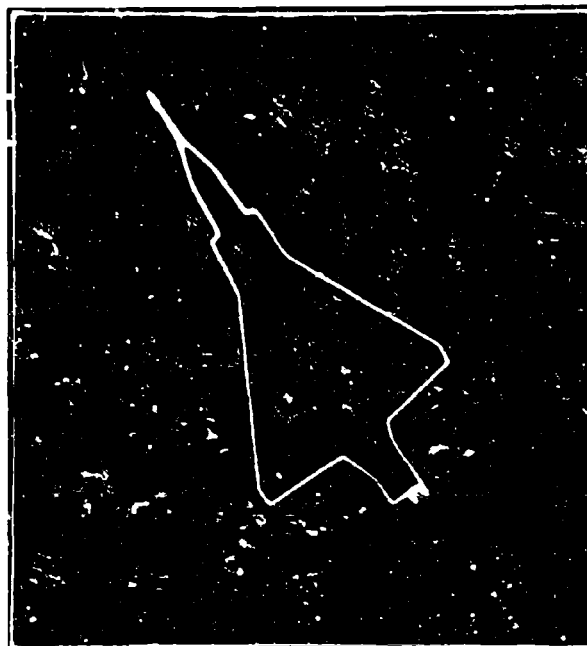
(a) $\psi = 5°$, $\phi = 75°$, $\theta = 55°$, $B = 7000$ ft., $A = C = 0$

(b) $\psi = 5°$, $\phi = 75°$, $\theta = -30°$, $B = 7000$ ft., $A = C = 0$

Figure 3.7   Perspective Projections for Different Elevation Angles

$$M_5 = (u_{30} - 3u_{12}) (u_{30} + u_{21}) [(u_{30} + u_{12})^2 - 3(u_{21} + u_{03})^2]$$

$$+ (3u_{21} - u_{03}) (u_{21} + u_{03}) \cdot [3(u_{30} + u_{12})^2 - (u_{21} + u_{03})^2]$$

$$(3-19)$$

$$M_6 = (u_{20} - u_{02}) [(u_{30} + u_{12})^2 - (u_{21} + u_{03})^2]$$

$$+ 4u_{11}(u_{30} + u_{12}) (u_{21} + u_{03})$$

$$(3-20)$$

3.6 Moment Invariance with Distance along Optical Axis

It is clear that as an object is moved along the optical axis, the first order effect on the image is just a change in size. The second order effect is that a few small portions of the image may appear or disappear when the object is moved along the optical axis. This second order effect diminishes as the distance of the object from the camera increases.

The radius of gyration, r, of a planar pattern is defined as follows:

$$r = (u_{20} + u_{02})^{\frac{1}{2}} \qquad (3-21)$$

The radius of gyration is directly proportional to the size of the image or inversely proportional to the distance of the object along the optical axis. The size of the image here is defined as the minimum radius of a circle required to enclose the given image completely

with its center at the centroid of the image. Thus the product RK of
the radius of gyration of the image and the distance along the optical
axis of the object is a constant.

$$RK = (u_{20} + u_{02})^{\frac{1}{2}} \cdot B \qquad (3-22)$$

Therefore the radius of gyration, r, should be used to normalize the
moment functions of Eqs. (3-15) through (3-20) to obtain the similitude
moment invariance. Using the results derived in section 2.5.3 con-
cerning similitude moment invariants, we have the following moment
functions invariant with the elevation angle θ and the distance B along
the optical axis:

$$M_2' = \frac{1}{r^4} [(u_{20} - u_{02})^2 + 4u_{11}^2] \qquad (3-23)$$

$$M_3' = \frac{1}{r^6} [(u_{30} - 3u_{12})^2 + (3u_{12} - u_{03})^2] \qquad (3-24)$$

$$M_4' = \frac{1}{r^6} [(u_{30} + u_{12})^2 + (u_{21} + u_{03})^2] \qquad (3-25)$$

$$M_5' = \frac{1}{r^{12}} [(u_{30} - 3u_{12})(u_{30} + u_{21})\{(u_{30} + u_{12})^2 - 3(u_{21} + u_{03})^2\}$$
$$+ (3u_{21} - u_{03})(u_{21} + u_{03})\{3(u_{30} + u_{12})^2 - (u_{21} + u_{03})^2\}]$$

$$(3-26)$$

$$M_6' = \frac{1}{r^8} \left[(u_{20} - u_{02}) \left\{ (u_{30} + u_{12})^2 - (u_{21} + u_{03})^2 \right\} \right.$$

$$\left. + 4u_{11}(u_{30} + u_{12})(u_{21} + u_{03}) \right] \qquad (3-27)$$

3.7 Elevation Bias Error

Let us consider a silhouette of an aircraft for a certain orientation as shown in Figure 3.8. Let this pattern have a principal axis as shown in the figure. This principal axis is the same as the perspective projection of the x axis of the coordinate system fixed to the center of gravity of the object or the aircraft in the present case. Therefore the inclination of this principal axis of the pattern with the U axis in the projection plane is the elevation angle θ. The positive direction of θ is shown in the figure.
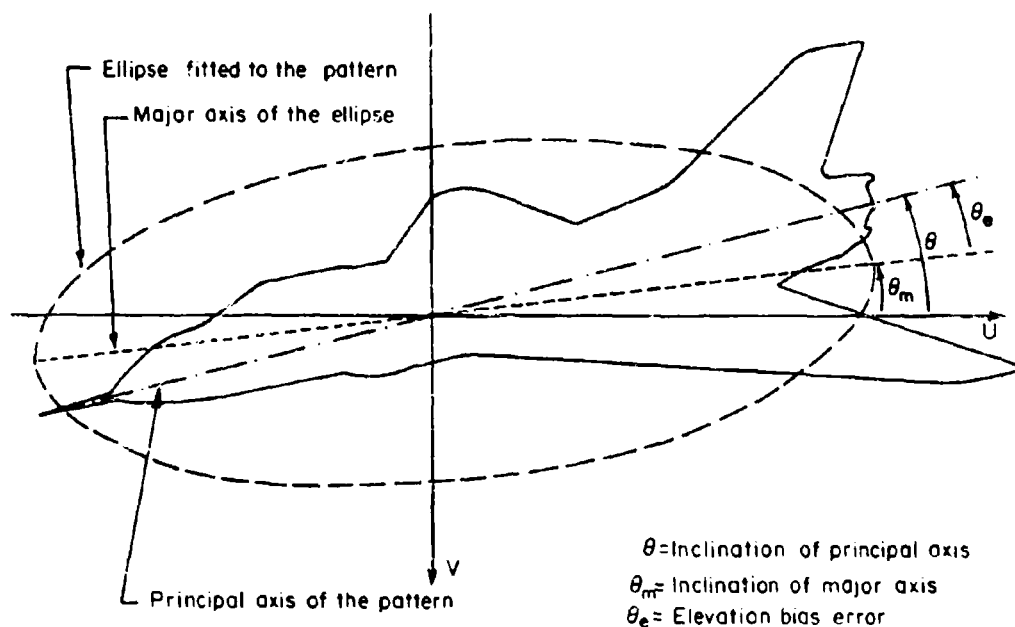
Figure 3.8 Elevation Bias Error for a Pattern

The inclination θ_m of the major axis of the ellipse fitted to the pattern can be found from Eq. (2-34), as shown below

$$\tan 2\theta_m = -2u_{11}/(u_{20} - u_{02}) \qquad (3-28)$$

with added restriction, such as $u_{20}' > u_{02}'$ and $u_{30}' > 0$, θ_m can be determined uniquely from Eq. (3-28).

The elevation bias error, θ_e, for a pattern as seen from Figure 3.8, is defined as the difference between the elevation angle θ and the inclination θ_m of the major axis of the ellipse fitted to the pattern.

$$\theta_e = \theta - \theta_m \qquad (3-29)$$

It is interesting to note here again that as the elevation angle is changed, the silhouette of the object just rotates in the projection plane and thus the elevation bias error, θ_e, remains constant for certain given values of the azimuth angle ψ, the roll angle ϕ and the distance B along the optical axis. Since the first order effect on the silhouette, when moving the object along the optical axis is just a change in size, we can say that the elevation bias error is nearly invariant with the distance B along the optical axis.

3.8 Sample Set Construction

In sections 3.5 and 3.6, we have derived five different functions of moments of the planar pattern, which are invariant with the

elevation angle θ and the distance B along the optical axis of the object to be identified. Thus, these five functions of moments can be used to provide a parametric representation of the silhouette of the object for given values of the azimuth and roll angles in a five-dimensional vector space. The moment functions M_2, M_3, M_4, M_5 and M_6 of Eqs. (3-23) through (3-27) are of different orders. Invariant moment functions of the same order should be used for the parametric representation of the silhouette in order to give equal weight or the same importance to each parameter used in the recognition pro- cedure. Therefore, let

$$\rho_1 = M_2' \tag{3-30}$$

$$\rho_2 = (M_3')^{4/6} \tag{3-31}$$

$$\rho_3 = (M_4')^{4/6} \tag{3-32}$$

$$\rho_4 = (M_5')^{4/12} \tag{3-33}$$

$$\rho_5 = (M_6')^{4/8} \tag{3-34}$$

and then, the vector $\vec{\rho} = (\rho_1, \rho_2, \rho_3, \rho_4, \rho_5)$ represents the given sil- houette in a five dimensional vector space.

A simulation program for obtaining the silhouette of a given object for any translation and orientation [26] is used here for con- struction of the sample set. The possible range of variations of the azimuth angle ψ and the roll angle ϕ are discretized; and then for all

of the different combinations of these discretized values of the two
angles with the values of A and C taken as zero, silhouettes are
generated from which the parameters o_1, ρ_2, ρ_3, ρ_4, ρ_5, the constant
RK, and the elevation bias error θ_e are computed. Thus a sample set
is constructed for a certain object and then repeated the same way
for the other objects to be identified.

3.9 Nearest Neighbor Rule for the Identification and Estimation of the Parameters

Let the vector $\vec{\rho}_i$ represent the ith pattern in a five dimensional
vector space from the sample set $(\vec{\rho}_1, n_1), \ldots \ldots, (\vec{\rho}_n, n_n)$ where the
n_i's take values in the set $\{1, 2, \ldots, K\}$. Each n_i is considered
to be the index of the category to which the ith individual belongs,
and each $\vec{\rho}_i$ is the outcome of the set of measurements made upon that
individual pattern. For brevity, we can say "$\vec{\rho}_i$ belongs to n_i" when
we precisely mean that the ith individual, upon which measurements $\vec{\rho}_i$
have been made, belongs to category n_i.

A new pair $(\vec{\rho}, n)$ is given, where only the measurement $\vec{\rho}$ is
made, and it is desired to estimate n by utilizing the information con-
tained in the sample set of correctly classified vectors. We shall
call

$$\vec{\rho}' \, \epsilon \left\{ \vec{\rho}_1, \, \vec{\rho}_2, \, \ldots, \, \vec{\rho}_n \right\}$$

a nearest neighbor [29] to $\vec{\rho}$ if

$$\min d(\vec{\rho}_i, \vec{\rho}) = d(\vec{\rho}', \vec{\rho}) \quad i=1,2, \ldots n. \qquad (3\text{-}35)$$

The unknown input $\vec{\rho}$, by the nearest neighbor rule, belongs to the category or the class η' of its nearest neighbor $\vec{\rho}'$ defined in Eq. (3-35). A mistake is made when $\eta' \neq \eta$. The nearest neighbor rule described here utilizes only the classification of the nearest neighbor. The remaining n-1 classifications are ignored.

The computations involved in this approach are fairly simple. An alternative approach using linear separatibility of the sample set into different classes could possibly be used for the identification, but then the computations involved would be more complex and difficult.

3.10 Summary

In this chapter we first considered the mathematical representation of the object to be identified and of the optical system. Some functions of moments which are invariant with the elevation angle θ and the distance B along the optical axis were used to characterize the silhouette for the given values of the azimuth angle ψ and the roll angle ϕ. A procedure was then described to form the sample set; then using this sample set a nearest neighbor rule useful for the identification and the estimation of the parameters of the unknown object was discussed.

CHAPTER IV

COMPUTATIONAL RESULTS

4.1 Introduction

Wire Frame structure representation of three different aircraft, a F-4B Phantom II, a Mirage IIIC, and a MIG 21 is presented in this chapter. The moment functions which are invariant with the elevation angle and the distance along the optical axis, derived in Chapter III, are then analyzed. Using the parametric representation of the silhouettes generated, the construction of the sample set for the three aircraft considered is shown. The results obtained by the application of the nearest neighbor rule described in Chapter III for the identification and estimation of parameters are presented later in this chapter. The effect of noise on identification and estimation is also studied.

4.2 Wire Frame Structure Representation

Prototype models of scale 1:72 are used for the purpose of obtaining the wire frame structure representation of the three different aircraft considered. A number of points called nodes are selected on the body of the prototype to represent the three dimensional objects, or the aircraft, in the present case. The number of nodes required and their positions on the body of the prototype for a complete and fair representation of the three dimensional object depends on the object's

42

complexity. It is obvious that the number of nodes necessary to represent a curved surface would be more than that necessary to represent a planar surface. The computation time required to generate the silhouette for a certain given translation and rotation increases more than linearly with the number of nodes selected.

The coordinates of the 79 nodes selected on the Phantom F-4B aircraft, with respect to the center of gravity of the aircraft, appear in Table I. The connection matrix for these nodes selected is given in Table II.

TABLE 1

COORDINATES OF THE NODES FOR THE PHANTOM AIRCRAFT
(With Respect to Its Center of Gravity and in Feet)

Node	x	y	z
1	4.46	-1.37	5.21
2	4.46	1.37	5.21
3	26.04	-2.03	-0.92
4	26.04	2.03	-0.92
5	26.04	-2.03	1.33
6	26.04	2.03	1.33
7	18.32	-2.96	-2.20
8	18.32	2.96	-2.20
9	18.32	-3.75	-2.01
10	18.32	3.75	-2.01
11	17.85	-3.75	2.06
12	17.85	3.75	2.06
13	17.61	-2.59	2.49
14	17.61	2.59	2.49
15	10.28	-2.44	-2.49
16	10.28	2.44	-2.49
17	10.28	-4.29	-1.67
18	10.28	4.29	-1.67
19	13.21	-4.53	1.83
20	13.21	4.53	1.83
21	3.50	-4.53	1.83

TABLE 1--Continued

Node	x	y	z
22	3.50	4.5	1.83
23	3.5	-4.53	3.03
24	3.50	4.53	3.03
25	-1.32	-4.29	-1.20
26	-1.32	4.29	-1.20
27	-5.28	-4.53	2.52
28	-5.28	4.53	2.52
29	-1.44	-12.56	2.67
30	-1.44	12.56	2.67
31	-1.44	-12.56	3.27
32	-1.44	12.56	3.27
33	3.56	-12.56	2.48
34	3.56	12.56	2.48
35	-6.45	-12.56	2.85
36	-6.45	12.56	2.85
37	-4.22	-19.51	1.64
38	-4.22	19.51	1.64
39	-7.63	-19.51	1.64
40	-7.63	19.51	1.64
41	-6.66	-3.30	-2.41
42	-6.66	3.30	-2.41
43	-9.47	-3.52	-0.64
44	-9.47	3.52	-0.64
45	-9.04	-4.26	0.17
46	-9.04	4.26	0.17
47	-9.04	-3.78	3.02
48	-9.04	3.78	3.02
49	-14.89	-2.27	-2.15
50	-14.89	2.27	-2.15
51	-19.36	-1.89	-2.43
52	-19.36	1.89	-2.43
53	-19.36	-1.89	-1.83
54	-19.36	1.89	-1.83
55	-22.66	-1.47	-1.80
56	-22.66	1.47	-1.80
57	-20.98	-11.50	-1.10
58	-20.98	11.50	-1.10
59	-22.90	-11.50	-1.10
60	-22.90	11.50	-1.10
61	-14.69	-0.60	-3.98
62	-14.69	0.60	-3.98
63	34.43	0.00	1.04
64	26.04	0.00	-1.62
65	26.04	0.00	2.49

TABLE 1--Continued

Node	x	y	z
66	22.36	0.00	-3.72
67	18.04	0.00	-4.50
68	13.21	0.00	2.49
69	-13.21	0.00	-3.98
70	-6.66	0.00	-3.98
71	-22.97	0.00	-3.10
72	-18.52	0.00	-9.58
73	-22.78	0.00	-9.75
74	-23.48	0.00	-2.28
75	-9.04	0.00	2.49
76	10.70	0.00	2.49
77	14.87	0.00	4.44
78	-5.99	0.00	4.44
79	4.70	0.00	2.49

TABLE 2

CONNECTION MATRIX FOR THE PHANTOM AIRCRAFT

Node	Nodes Connected To						
1	76	79	77	78	0	0	0
2	76	79	77	78	0	0	0
3	63	64	5	66	7	0	0
4	63	64	6	66	8	0	0
5	63	65	3	13	0	0	0
6	63	65	4	14	0	0	0
7	69	15	66	9	3	13	0
8	69	16	66	10	4	14	0
9	7	11	17	19	0	0	0
10	8	12	18	20	0	0	0
11	9	13	19	0	0	0	0
12	10	14	20	0	0	0	0
13	7	11	5	68	0	0	0
14	8	12	6	68	0	0	0
15	17	7	69	41	25	0	0
16	18	8	69	42	26	0	0
17	15	19	9	25	21	0	0

TABLE 2--<u>Continued</u>

Node	Nodes Connected To						
18	16	20	10	26	22	0	0
19	11	17	21	23	33	9	0
20	12	18	22	24	34	10	0
21	17	19	27	29	0	0	0
22	18	20	28	30	0	0	0
23	19	27	31	0	0	0	0
24	20	28	32	0	0	0	0
25	15	17	41	43	45	27	0
26	16	18	42	44	46	28	0
27	21	23	35	25	47	0	0
28	22	24	36	26	48	0	0
29	21	33	35	37	0	0	0
30	22	34	36	38	0	0	0
31	33	35	23	39	0	0	0
32	34	36	24	40	0	0	0
33	29	31	19	37	0	0	0
34	30	32	20	38	0	0	0
35	29	31	39	27	0	0	0
36	30	32	40	28	0	0	0
37	33	39	29	0	0	0	0
38	34	40	30	0	0	0	0
39	37	35	31	0	0	0	0
40	38	36	32	0	0	0	0
41	70	15	49	25	43	0	0
42	70	16	50	26	44	0	0
43	41	25	45	47	49	75	74
44	42	26	46	48	50	75	74
45	25	43	47	0	0	0	0
46	26	44	48	0	0	0	0
47	27	43	45	74	75	0	0
48	28	44	45	74	75	0	0
49	41	61	51	53	43	57	0
50	42	62	52	54	44	58	0
51	49	55	57	71	0	0	0
52	50	56	58	71	0	0	0
53	49	55	59	75	0	0	0
54	50	56	60	75	0	0	0
55	51	53	59	0	0	0	0
56	52	54	60	0	0	0	0
57	59	49	51	0	0	0	0
58	60	50	52	0	0	0	0
59	57	55	53	0	0	0	0

TABLE 2--<u>Continued</u>

Node	Nodes Connected To						
60	58	56	54	0	0	0	0
61	70	71	72	49	0	0	0
62	70	71	72	50	0	0	0
63	64	3	4	5	6	65	0
64	63	66	3	4	0	0	0
65	63	5	6	68	0	0	0
66	64	67	7	8	3	4	0
67	66	69	0	0	0	0	0
68	65	76	13	14	0	0	0
69	67	70	7	8	15	16	0
70	69	2	61	62	41	42	0
71	73	74	61	62	51	52	0
72	70	73	61	62	0	0	0
73	72	71	0	0	0	0	0
74	71	47	48	43	44	0	0
75	76	47	48	43	44	53	54
76	77	78	1	2	68	75	0
77	76	79	1	2	0	0	0
78	76	79	1	2	0	0	0
79	77	78	1	2	0	0	0

The trailing zeroes in the rows of the connection matrix of Table II show that no more nodes are connected to the node representing that row. For example, node 77 is only connected to the nodes 76, 79, 1 and 2.

Similar measurements were made for nodes selected for the other two aircraft. The body of the Mirage is less complex in shape than those of the Phantom and MIG aircraft, and therefore it is only necessary to select 59 nodes for the Mirage. The coordinates of the nodes and their connection matrix for the Mirage and MIG aircraft appear below in Tables III through VI.

TABLE 3

COORDINATES OF THE NODES FOR THE MIRAGE AIRCRAFT
(With Respect to Its Center of Gravity and in Feet)

Node	x	y	z
1	23.48	0.15	-0.02
2	23.48	-0.15	-0.02
3	18.62	1.56	-0.02
4	18.62	-1.56	-0.02
5	12.80	1.50	-3.95
6	12.80	-1.50	-0.95
7	12.80	2.76	-0.29
8	12.80	-2.76	-0.29
9	12.80	2.76	1.12
10	12.80	-2.76	1.12
11	12.80	1.50	1.51
12	12.80	-1.50	1.51
13	5.30	1.14	-1.76
14	5.30	-1.14	-1.76
15	6.11	2.73	-0.68
16	6.11	-2.73	-0.68
17	6.71	3.39	1.57
18	6.71	-3.39	1.57
19	-2.17	0.90	-1.58
20	-2.17	-0.90	-1.58
21	-2.59	1.74	-1.04
22	-2.59	-1.74	-1.07
23	-4.51	2.52	2.38
24	-4.51	-2.52	2.38
25	-10.42	12.63	3.25
26	-10.42	-12.63	3.25
27	-4.51	2.52	2.74
28	-4.51	-2.52	2.74
29	-11.11	0.33	-1.34
30	-11.11	-0.33	-1.34
31	-10.60	1.89	-0.23
32	-10.60	-1.89	-0.23
33	-13.18	3.09	2.38
34	-13.18	-3.09	2.38
35	-12.49	12.63	3.25
36	-12.49	-12.63	3
37	-16.93	1.62	1.01
38	-16.93	-1.62	1.81
39	-16.93	0.39	-0.71
40	-16.93	-0.39	-0.71
41	-20.17	1.83	0.79
42	-20.17	-1.83	0.79

TABLE 3--<u>Continued</u>

Node	x	y	z
43	-20.17	1.23	1.81
44	-20.17	-1.23	1.81
45	29.03	0.00	-0.02
46	23.48	0.00	-0.47
47	23.48	0.00	-0.17
48	18.62	0.00	-1.34
49	18.62	0.00	1.39
50	14.66	0.00	-2.93
51	12.80	0.00	1.93
52	10.76	0.00	-2.72
53	5.30	0.00	-2.39
54	-1.72	0.00	-1.97
55	-7.66	0.00	-2.69
56	-17.89	0.00	-7.19
57	-21.07	0.00	-7.19
58	-18.52	0.00	-1.37
59	-21.46	0.00	-1.07

TABLE 4

CONNECTION MATRIX FOR THE MIRAGE AIRCRAFT

Node	Nodes Connected To						
1	45	46	47	3	0	0	0
2	45	46	47	4	0	0	0
3	48	49	1	5	11	0	0
4	48	49	2	6	12	0	0
5	50	52	3	7	11	13	0
6	50	52	4	8	12	14	0
7	5	9	15	0	0	0	0
8	6	10	16	0	0	0	0
9	7	11	17	0	0	0	0
10	8	12	18	0	0	0	0
11	49	51	3	5	9	0	0
12	49	51	4	6	10	0	0

TABLE 4--Continued

Node	Nodes Connected To						
13	53	5	15	19	52	0	0
14	53	6	16	20	52	0	0
15	7	13	17	21	0	0	0
16	8	14	18	22	0	0	0
17	51	9	15	18	23	25	27
18	51	10	16	17	24	26	28
19	54	13	21	29	0	0	0
20	54	14	22	30	0	0	0
21	15	19	23	31	0	0	0
22	16	20	24	32	0	0	0
23	17	21	25	33	35	0	0
24	18	22	26	34	36	0	0
25	17	23	27	35	0	0	0
26	18	24	28	36	0	0	0
27	17	25	28	33	0	0	0
28	18	26	27	34	0	0	0
29	54	55	58	19	31	39	56
30	54	55	58	20	32	40	56
31	21	29	33	37	41	0	0
32	22	30	34	38	42	0	0
33	23	31	34	35	37	27	0
34	24	32	33	36	38	28	0
35	25	33	23	0	0	0	0
36	26	34	24	0	0	0	0
37	31	33	38	43	0	0	0
38	32	34	37	44	0	0	0
39	58	59	29	41	40	0	0
40	58	59	30	42	39	0	0
41	31	39	43	42	0	0	0
42	32	40	44	41	0	0	0
43	37	41	44	0	0	0	0
44	38	42	43	0	0	0	0
45	46	47	1	2	0	0	0
46	45	48	1	2	0	0	0
47	45	49	1	2	0	0	0
48	46	50	3	4	0	0	0
49	47	51	3	4	11	12	0
50	48	52	5	6	0	0	0
51	49	11	12	17	18	0	0
52	50	53	5	6	13	14	0
53	52	54	13	14	0	0	0

TABLE 4--<u>Continued</u>

Node	Nodes Connected To						
54	53	55	19	20	29	30	0
55	54	56	29	30	0	0	0
56	55	57	29	30	0	0	0
57	56	58	0	0	0	0	0
58	57	59	29	30	39	40	0
59	58	39	40	0	0	0	0

TABLE 5

COORDINATES OF THE NODES FOR THE MIG 21 AIRCRAFT
(With Respect to Its Center of Gravity and in Feet)

Node	x	y	z
1	30.13	1.20	0.37
2	30.13	-1.20	0.37
3	17.02	1.74	-1.43
4	17.02	-1.74	-1.43
5	17.02	1.74	0.61
6	17.02	-1.74	0.61
7	11.50	1.53	-2.51
8	11.50	-1.53	-2.51
9	11.50	1.98	0.37
10	11.50	-1.98	0.37
11	11.50	1.53	1.45
12	11.50	-1.50	1.45
13	8.83	2.70	0.37
14	8.83	-2.70	0.37
15	5.95	0.48	-2.09
16	5.95	-0.48	-2.12
17	5.95	1.59	-1.49
18	5.95	-1.59	-1.49
19	1.75	2.19	-0.47
20	1.75	-2.19	-0.47
21	1.75	2.19	0.61
22	1.75	-2.19	0.61
23	1.75	1.53	1.42
24	1.75	-1.53	1.42

TABLE 5--Continued

Node	x	y	z
25	1.75	1.02	3.85
26	1.75	-1.02	3.85
27	-4.97	0.48	-2.09
28	-4.97	-0.48	-2.09
29	-4.97	1.59	-1.49
30	-4.97	-1.59	-1.49
31	-7.70	12.87	0.37
32	-7.70	-12.87	0.37
33	-9.14	12.87	0.37
34	-9.14	-12.87	0.37
35	-9.14	2.22	0.37
36	-9.14	-2.22	0.37
37	-13.01	0.72	-2.00
38	-13.01	-0.72	-2.00
39	-13.01	1.74	-1.07
40	-13.01	-1.74	-1.07
41	-13.01	2.01	0.37
42	-13.01	-2.01	0.37
43	-13.01	1.74	1.42
44	-13.01	-1.74	1.42
45	-16.58	1.62	0.37
46	-16.58	-1.62	0.37
47	-20.00	6.21	0.37
48	-20.00	-6.21	0.37
49	-18.92	6.54	0.37
50	-18.92	-6.54	0.37
51	-23.27	6.54	0.37
52	-23.27	-6.54	0.37
53	-19.97	1.50	0.37
54	-19.97	-1.50	0.37
55	30.91	-0.00	0.37
56	30.13	-0.00	1.57
57	17.05	-0.00	-2.39
58	13.69	-0.00	-3.95
59	5.95	-0.00	-2.15
60	-4.97	-0.00	-2.15
61	-9.56	-0.00	-3.20
62	-19.76	-0.00	-7.46
63	-24.68	-0.00	-7.46
64	-19.10	-0.00	-1.22
65	-19.97	-0.00	-1.07
66	-19.97	-0.00	1.69
67	-9.17	-0.00	3.55

TABLE 5--Continued

Node	x	v	z
68	-7.88	-0.00	2.32
69	1.75	-0.00	2.32
70	1.75	-0.00	3.01
71	-6.32	-0.00	3.85
72	1.75	-0.00	4.69
73	11.59	-0.00	3.85
74	11.50	-0.00	2.32
75	17.02	-0.00	1.90
76	27.13	-0.00	-0.05
77	33.13	-0.00	2.32
78	28.63	-0.00	-0.35
79	30.13	-0.00	-0.83

TABLE 6

CONNECTION MATRIX FOR THE MIG 21 AIRCRAFT

Node	Nodes Connected To						
1	55	56	79	3	5	0	0
2	55	56	79	4	6	0	0
3	57	1	5	7	0	0	0
4	57	2	6	8	0	0	0
5	75	1	3	9	11	0	0
6	75	2	4	10	12	0	0
7	58	3	9	15	0	0	0
8	58	4	10	16	0	0	0
9	5	7	11	13	17	19	21
10	6	8	12	14	18	20	22
11	74	5	9	23	0	0	0
12	74	6	10	24	0	0	0
13	9	19	21	31	0	0	0
14	10	20	22	32	0	0	0
15	59	7	17	27	0	0	0
16	59	8	18	28	0	0	0
17	9	15	19	29	0	0	0
18	10	16	20	30	0	0	0
19	9	13	17	31	35	0	0
20	10	14	18	32	36	0	0

TABLE 6--Continued

Node	Nodes Connected To						
21	9	13	23	31	35	0	0
22	10	14	24	32	36	0	0
23	69	11	21	43	0	0	0
24	69	12	22	44	0	0	0
25	70	71	72	73	0	0	0
26	70	71	72	73	0	0	0
27	60	15	29	37	0	0	0
28	60	16	30	38	0	0	0
29	17	27	35	39	0	0	0
30	18	28	36	40	0	0	0
31	13	19	21	33	0	0	0
32	14	20	22	34	0	0	0
33	31	35	0	0	0	0	0
34	32	36	0	0	0	0	0
35	19	21	29	33	39	41	43
36	20	22	30	34	40	42	44
37	61	62	64	27	39	0	0
38	61	62	64	28	40	0	0
39	64	65	29	35	37	41	53
40	64	65	30	36	38	42	54
41	35	39	43	45	47	0	0
42	36	40	44	46	48	0	0
43	66	68	23	35	41	53	0
44	66	68	24	36	42	54	0
45	41	53	0	0	0	0	0
46	42	54	0	0	0	0	0
47	41	49	51	0	0	0	0
48	42	50	52	0	0	0	0
49	47	51	0	0	0	0	0
50	48	52	0	0	0	0	0
51	47	49	53	0	0	0	0
52	48	50	54	0	0	0	0
53	65	66	39	43	45	51	0
54	65	66	40	44	46	52	0
55	56	79	1	2	0	0	0
56	55	57	1	2	0	0	0
57	56	58	3	4	0	0	0
58	57	59	7	8	0	0	0
59	58	60	15	16	0	0	0
60	59	61	27	28	0	0	0
61	60	62	37	38	0	0	0
62	61	63	37	38	0	0	0
63	62	64	0	0	0	0	0

TABLE 6--Continued

Node	Nodes Connected To						
64	63	65	37	38	39	40	0
65	64	39	40	53	54	0	0
66	67	68	43	44	53	54	0
67	66	68	0	0	0	0	0
68	66	67	69	43	44	0	0
69	68	74	23	24	0	0	0
70	71	73	25	26	0	0	0
71	70	72	25	26	0	0	0
72	71	73	25	26	0	0	0
73	70	72	25	26	0	0	0
74	69	75	11	12	0	0	0
75	74	76	5	6	0	0	0
76	75	77	78	0	0	0	0
77	76	78	0	0	0	0	0
78	76	77	79	0	0	0	0
79	55	78	1	2	0	0	0

4.3 Generation of Data Points

It is desired to represent the given silhouette of a certain object by some finite number of points called data points. These data points are used for the calculation of moments for the given silhouette. The most realistic situation about the existence of these data points is perhaps to have them uniformly distributed along the silhouette or the boundary of the optical image. The subroutine that generated these data points is called DATA.

Let UVLE be the distance between any two adjacent data points on the silhouette or the boundary. The number of data points generated for a given silhouette is inversely proportional to the distance UVLE; and therefore as the distance UVLE is decreased, the computation time

required for the moment calculations is increased. However, by de-
creasing the distance UVLE, one can obtain a more faithful discrete
representation of the given continuous silhouette. A compromise for
the value of UVLE, on the basis of the computation time and the
accuracy desired, is made.

For a certain given silhouette, the variation in the values of
the parameter ρ_3 of Eq. (3-32) with the distance UVLE is shown in
Figure 4.1. The parameter ρ_3 varies considerably for values of UVLE
greater than 0.0003 inch and remains nearly constant for values of
UVLE less than 0.0003 inch. This shows that for values of UVLE for
which any of the parameters ρ_1, ρ_2, ρ_3, ρ_4 or ρ_5 remain nearly constant,
we have a comparatively more exact and fair representation of the given
continuous silhouette. A compromise, on the basis of the computer core
available, the computation time and the accuracy desired, is made for
UVLE equal to 0.0002 inch.
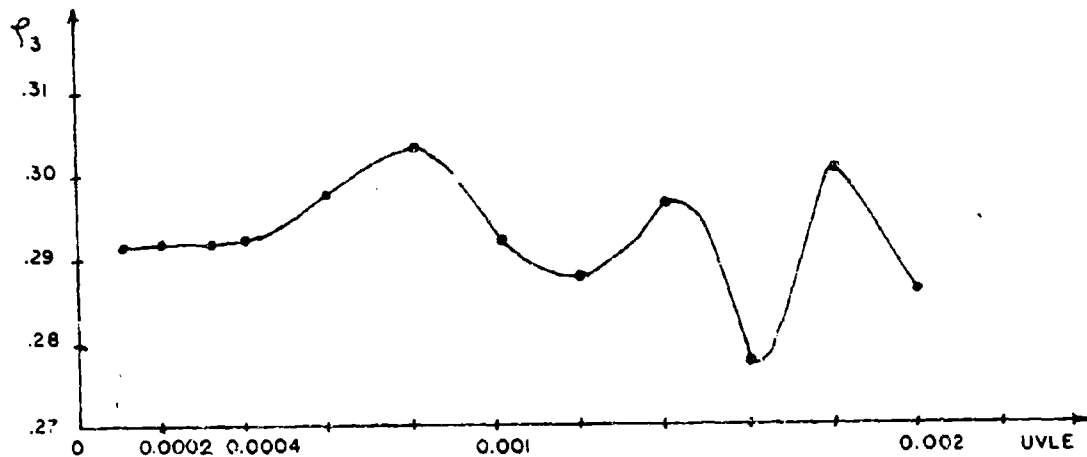
Figure 4.1 Variation of the Parameter ρ_3 with UVLE

4.4 Moment Invariance with the Angle of Elevation

It was shown in Chapter III that the vector $\vec{\rho} = (\rho_1, \rho_2, \rho_3, \rho_4, \rho_5)$, where the parameters $\rho_1, \rho_2, \rho_3, \rho_4$ and ρ_5 are functions of moments which are invariant with the elevation angle θ and the distance B along the optical axis, characterizes a silhouette with given azimuth and roll angles. The invariance of one of these five parameters, ρ_1, with the elevation angle is shown in Table VII. Similar results hold for the other parameters also.

TABLE 7

VARIATION OF THE PARAMETER ρ_1 WITH THE ELEVATION ANGLE
AIRCRAFT: MIRAGE, B = 7000 ft., ψ = 10°, ϕ = 20°

θ in degrees	A = C =0 ft.	A = C =50 ft.	A = C =100 ft.
-90.0	0.8158	0.8142	0.8142
-75.0	0.8158	0.8142	0.8142
-60.0	0.8158	0.8146	0.8146
-45.0	0.8158	0.8153	0.8153
-30.0	0.8158	0.8158	0.8158
-15.0	0.8158	0.8166	0.8166
0.0	0.8158	0.8171	0.8171
15.0	0.8158	0.8175	0.8175
30.0	0.8158	0.8177	0.8177
45.0	0.8158	0.8179	0.8179
60.0	0.8158	0.8183	0.8183
75.0	0.8158	0.8182	0.8182
90.0	0.8158	0.8180	0.8180

It is seen from Table VII that the value of the parameter ρ_1 does not vary with the elevation angle θ for the case when the center of gravity of the object to be identified lies on the optical axis. For the other two cases where the center of gravity is off the optical axis,

there is a slight variation of less than 1% in the value of the
parameter o_1. For the present case, it is reasonable to assume the
maximum value of the off-axis distances A and C to be about 30 ft. only,
as for values greater than this the aircraft, with our present consid-
erations, will not be completely in view. This is shown in Figure 4.2
where the silhouette is generated for the off-axis distances A and C
equal to 25 ft., and the optical axis distance B equal to 10,000 ft.
This maximum value for the off-axis distances A and C will obviously
decrease when smaller optical axis distances are considered.

4.5 Moment Invariance with Distance Along the Optical Axis

It was stated in the last chapter that the radius of gyration of
the optical image or the silhouette is inversely proportional to the
distance of the object along the optical axis, and hence the product RK
of the radius of gyration and the distance along the optical axis re-
mains constant. This is shown to be valid from the computational re-
sults shown in Table VIII.

The fact that the product RK remains nearly invariant with the
distance along the optical axis was used in Chapter III to normalize
some of the moment functions to obtain their invariance in relation to
the distance along the optical axis. The variation of one of the
parameters o_4 with the distance B is shown in Table IX.

4.6 Sample Set Construction

A simulation program which appears in Appendix I is used to gen-
erate the silhouette of an object, given its three translational and
three rotational parameters. The possible range of variation of the
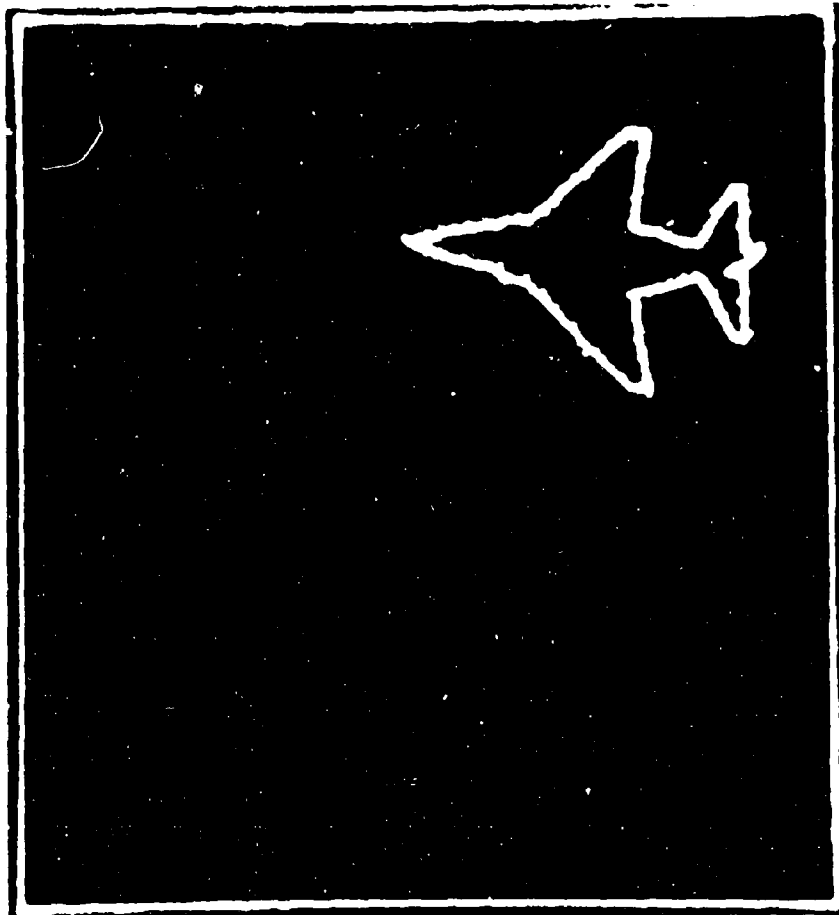
Figure 4.2 Perspective View of Phantom with Off-Axis
Distances A = C = 25 ft., B = 10000 ft., ψ = 5°, ϕ = 75°, θ = 10°

TABLE 8

VARIATION OF $KK = (u_{20} + u_{02})^{\frac{1}{2}} \cdot B$ WITH DISTANCE B

AIRCRAFT: PHANTOM, $\psi = 5°$, $\phi = 75°$, $\theta = 10°$

B in feet	A = C =0 ft.	A = C =10 ft.	A = C =20 ft.
5000.0	2738.8	2738.4	2737.9
5500.0	2739.9	2739.4	2738.7
6000.0	2740.2	2739.9	2739.2
6500.0	2739.2	2740.0	2739.9
7000.0	2740.0	2739.6	2740.0
7500.0	2739.1	2740.2	2740.3
8000.0	2740.2	2739.8	2739.6
8500.0	2740.6	2740.3	2740.3
9000.0	2739.1	2739.1	2738.2
9500.0	2739.2	2738.9	2738.7
10000.0	2740.7	2740.4	2740.2
10500.0	2739.6	2739.4	2739.1
11000.0	2740.3	2740.0	2740.2
11500.0	2741.1	2742.7	2742.5
12000.0	2737.9	2737.7	2737.5

TABLE 9

VARIATION OF THE PARAMETER ρ_4 WITH THE DISTANCE B

AIRCRAFT: PHANTOM, $\psi = 5°$, $\phi = 75°$, $\theta = 10°$

B in feet	A = C =0 ft.	A = C =10 ft.	A = C = 20 ft.
5000.0	0.2076	0.2077	0.2081
5500.0	0.2086	0.2081	0.2077
6000.0	0.2089	0.2087	0.2083
6500.0	0.2065	0.2068	0.2071
7000.0	0.2086	0.2086	0.2087
7500.0	0.2082	0.2074	0.2080
8000.0	0.2078	0.2077	0.2063
8500.0	0.2073	0.2072	0.2077
9000.0	0.2082	0.2079	0.2079
9500.0	0.2065	0.2064	0.2064
10000.0	0.2095	0.2095	0.2095
10500.0	0.2063	0.2063	0.2062
11000.0	0.2075	0.2074	0.2081
11500.0	0.2071	0.2074	0.2073
12000.0	0.2085	0.2084	0.2084

azimuth angle ψ and the roll angle ϕ are 0 to 360 degrees. But because of the symmetry of the aircraft about their major axis or the x-axis of the coordinate system fixed to the center of gravity, the silhouettes for the four roll angles ϕ, 180 -ϕ, 180 +ϕ and 360 -ϕ will be almost similar. Thus we will expect the parameters ρ_1, ρ_2, ρ_3, ρ_4 and ρ_5 to have nearly the same values for all the four angles mentioned above; and therefore the same vector $\vec{\rho} = (\rho_1, \rho_2, \rho_3, \rho_4, \rho_5)$ will represent the four silhouettes for these roll angles, with the same azimuth angles. This is shown in the Figure 4.3.
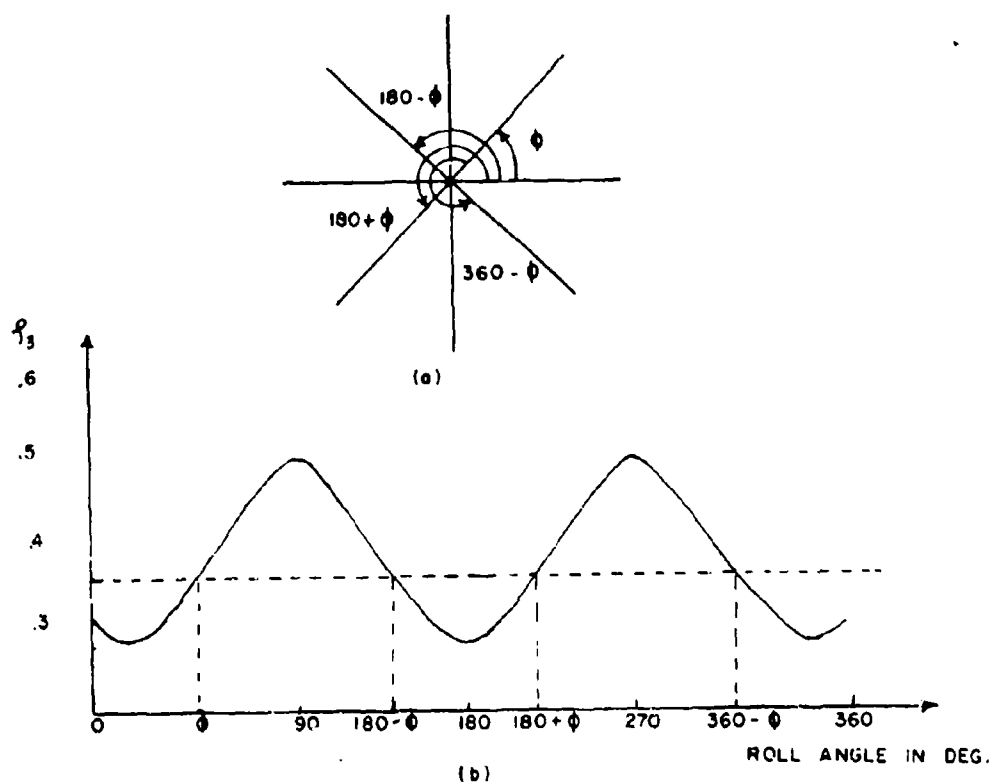
Figure 4.3 Representation of the Four Different Roll Angles
having similar Silhouettes

The same considerations apply to the azimuth angle also. Making use of these symmetric properties of the roll and azimuth angles, we may consider the variations of ϕ and ψ from 0 to 90 degrees only. The range of variations of the azimuth and roll angles are discretized at an interval of 5 degrees each; and then for all of the different combinations of these discretized values of the two angles with A and C taken as zero, silhouettes are generated from which the parameters ρ_1, ρ_2, ρ_3, ρ_4, ρ_5, the constant RK, and the elevation bias error θ_e are computed. Thus the whole sample set consisting of 361 pattern vectors for each aircraft is constructed. Tables X and XI give the sample set for the Phantom and Mirage aircraft respectively. The variations for ψ and ϕ in these tables appear in steps of 15 degrees, but these tables were computed in steps of 5 degree variations.

4.7 Identification and Estimation of the Parameters

The Nearest Neighbor Rule described in Chapter III is used for the identification and estimation of the three translational and the three rotational parameters. The sample set $(\vec{\rho}_1, \eta_1)$, $(\vec{\rho}_2, \eta_2)$ ... $(\vec{\rho}_n, \eta_n)$ is stored in the computer; and then for an unknown pattern vector $\vec{\rho}$, its nearest neighbor defined in Eq. (3-35) is searched. This is done by using the subroutine ESTM, given in Appendix I.

4.7.1 Identification of the Unknown Object

Let the nearest neighbor of the unknown pattern vector $\vec{\rho}$ be $(\vec{\rho}', \eta')$. We may therefore say that $\vec{\rho}$ belongs to η'. The information contained in η' is the class of the object, the azimuth and roll angles,

TABLE 10

SAMPLE SET CONSTRUCTION FOR PHANTOM

A = C = 0, B = 7000 feet

ψ	φ	ρ₁	ρ₂	ρ₃	ρ₄	ρ₅	RK	EB
0.0	0.0	0.7924	0.1527	0.0365	0.0466	0.0670	2465.1	-5.42
0.0	15.0	0.7813	0.1303	0.0379	0.0377	0.0368	2588.3	-4.04
0.0	30.0	0.6718	0.2363	0.1210	0.1428	0.1800	2607.2	-2.36
0.0	45.0	0.5076	0.2916	0.1552	0.1816	0.2077	2648.1	-1.40
0.0	60.0	0.3682	0.3344	0.1765	0.2069	0.2119	2704.3	-1.10
0.0	75.0	0.2850	0.3504	0.1808	0.2133	0.2026	2739.2	-0.52
0.0	90.0	0.2719	0.3589	0.2101	0.2402	0.2241	2747.6	-0.11
15.0	0.0	0.7949	0.1273	0.0350	0.0268	0.0436	2456.4	-5.21
15.0	15.0	0.7642	0.1747	0.0779	0.0915	0.1196	2547.6	-3.04
15.0	30.0	0.6556	0.2640	0.1428	0.1664	0.2052	2575.3	-0.79
15.0	45.0	0.4938	0.2881	0.1616	0.1866	0.2134	2612.7	0.67
15.0	60.0	0.3572	0.3072	0.1745	0.2008	0.2087	2661.3	1.06
15.0	75.0	0.2718	0.3104	0.1736	0.2007	0.1941	2692.6	0.76
15.0	90.0	0.2608	0.3151	0.2002	0.2242	0.2138	2700.5	0.03
30.0	0.0	0.7704	0.1515	0.0810	0.0908	0.1189	2284.6	-4.71
30.0	15.0	0.7232	0.2552	0.1497	0.1694	0.2139	2377.8	-1.97
30.0	30.0	0.6068	0.3110	0.1748	0.2015	0.2364	2404.8	0.99
30.0	45.0	0.4341	0.2998	0.1744	0.1995	0.2190	2439.3	3.00
30.0	60.0	0.2911	0.2743	0.1674	0.1890	0.1918	2481.0	3.71
30.0	75.0	0.2068	0.2530	0.1601	0.1794	0.1704	2511.0	2.59
30.0	90.0	0.1946	0.2464	0.1777	0.1928	0.1818	2518.7	-0.31
45.0	0.0	0.7130	0.2137	0.1715	0.1798	0.2378	2030.3	-3.95
45.0	15.0	0.6431	0.3491	0.2262	0.2507	0.2913	2079.6	-0.45
45.0	30.0	0.5012	0.3643	0.2031	0.2349	0.2544	2103.1	3.81
45.0	45.0	0.3211	0.2975	0.1707	0.1958	0.1991	2147.9	7.73
45.0	60.0	0.1796	0.2115	0.1422	0.1558	0.1402	2191.5	3.68
45.0	75.0	0.0983	0.1520	0.1275	0.1327	0.1180	2221.9	7.48
45.0	90.0	0.0782	0.1302	0.1351	0.1338	0.1178	2227.2	1.07

TABLE 10—Continued

η	φ	ρ_1	ρ_2	ρ_3	ρ_4	ρ_5	RK	EB
60.0	0.0	0.5970	0.2045	0.2013	0.1981	0.2633	1626.4	-2.83
60.0	15.0	0.5129	0.3688	0.2302	0.2564	0.2812	1710.1	3.61
60.0	30.0	0.3697	0.3436	0.1614	0.1949	0.1952	1750.4	11.72
60.0	45.0	0.2174	0.2613	0.1228	0.1463	0.1325	1805.2	21.03
60.0	60.0	0.0956	0.1522	0.0949	0.0975	0.0774	1851.6	30.50
60.0	75.0	0.0236	0.0637	0.0808	0.0482	0.0331	1879.5	40.26
60.0	90.0	0.0008	0.0143	0.0748	0.0479	0.0194	1887.0	****
75.0	0.0	0.6154	0.2949	0.1543	0.1803	0.2086	1523.5	-2.79
75.0	15.0	0.5390	0.3282	0.1481	0.1793	0.1989	1531.7	10.47
75.0	30.0	0.4445	0.3167	0.0862	0.1169	0.1046	1530.7	24.89
75.0	45.0	0.3480	0.3194	0.0765	0.0994	0.0689	1551.5	39.41
75.0	60.0	0.2818	0.3073	0.0632	0.0645	0.0193	1578.3	****
75.0	75.0	0.2325	0.2847	0.0494	0.0607	0.0597	1593.8	****
75.0	90.0	0.2208	0.2763	0.0446	0.0689	0.0652	1598.7	-6.01
90.0	0.0	0.6384	0.2812	0.0636	0.0854	0.0621	1461.3	-1.25
90.0	15.0	0.6083	0.2851	0.0508	0.0609	0.0122	1456.1	13.71
90.0	30.0	0.5975	0.2869	0.0472	0.0489	0.0362	1453.5	18.76
90.0	45.0	0.5420	0.3018	0.0426	0.0381	0.0562	1456.6	43.95
90.0	60.0	0.5191	0.3156	0.0425	0.0553	0.0665	1461.5	****
90.0	75.0	0.5074	0.3172	0.0402	0.0635	0.0721	1464.2	****
90.0	90.0	0.5028	0.3229	0.0401	0.0674	0.0753	1463.9	-5.14

TABLE 11

SAMPLE SET CONSTRUCTION FOR MIRAGE

A = C = 0, B = 7000 feet

ψ	φ	ρ₁	ρ₂	ρ₃	ρ₄	ρ₅	RK	EB
0.0	0.0	0.8935	0.1490	0.0916	0.1030	0.1575	2298.2	-2.49
0.0	15.0	0.8413	0.1994	0.1051	0.1225	0.1687	2304.8	-1.49
0.0	30.0	0.7844	0.2366	0.1008	0.1234	0.1575	2304.4	-0.22
0.0	45.0	0.6873	0.2713	0.0934	0.1216	0.1492	2293.5	0.39
0.0	60.0	0.5938	0.3110	0.0999	0.1327	0.1553	2298.9	0.66
0.0	75.0	0.5181	0.3390	0.0866	0.1218	0.1355	2294.3	0.82
0.0	90.0	0.4852	0.3601	0.0793	0.1158	0.1247	2292.0	-0.00
15.0	0.0	0.8782	0.2032	0.1351	0.1493	0.2126	2227.5	-2.05
15.0	15.0	0.8270	0.2459	0.1379	0.1588	0.2103	2239.6	-1.07
15.0	30.0	0.7655	0.2835	0.1310	0.1582	0.1968	2249.6	0.03
15.0	45.0	0.6740	0.3013	0.1183	0.1494	0.1804	2245.8	0.85
15.0	60.0	0.5829	0.3110	0.1122	0.1446	0.1692	2246.9	1.29
15.0	75.0	0.5146	0.3185	0.1043	0.1378	0.1554	2249.3	1.09
15.0	90.0	0.4746	0.3286	0.0826	0.1166	0.1279	2234.0	-0.00
30.0	0.0	0.8430	0.2788	0.1902	0.2090	0.2743	2027.8	-1.43
30.0	15.0	0.7872	0.3269	0.1865	0.2143	0.2647	2048.9	-0.35
30.0	30.0	0.7123	0.3205	0.1330	0.1656	0.2004	2008.0	0.88
30.0	45.0	0.6209	0.3561	0.1426	0.1792	0.2049	2066.2	1.57
30.0	60.0	0.5248	0.3347	0.1304	0.1644	0.1846	2067.1	2.02
30.0	75.0	0.4553	0.3064	0.1161	0.1476	0.1633	2070.3	1.55
30.0	90.0	0.4126	0.2951	0.0821	0.1130	0.1249	2058.9	-0.00
45.0	0.0	0.7729	0.3607	0.2368	0.2628	0.3182	1720.4	-0.38
45.0	15.0	0.6989	0.4392	0.2271	0.2676	0.3006	1738.4	1.10
45.0	30.0	0.6084	0.4892	0.2046	0.2544	0.2680	1751.7	2.20
45.0	45.0	0.4962	0.4445	0.1556	0.2017	0.2078	1761.1	3.41
45.0	60.0	0.3899	0.3523	0.1193	0.1544	0.1602	1768.8	3.96
45.0	75.0	0.3122	0.2650	0.0951	0.1216	0.1278	1776.9	2.83
45.0	90.0	0.2707	0.2305	0.0669	0.0912	0.0949	1771.5	0.00

TABLE 11--Continued

ψ	φ	ρ_1	ρ_2	ρ_3	ρ_4	ρ_5	RK	EB
60.0	0.0	0.6282	0.3807	0.1924	0.2279	0.2552	1347.0	1.80
60.0	15.0	0.5231	0.5785	0.2074	0.2680	0.2560	1357.3	4.81
60.0	30.0	0.4435	0.5332	0.0912	0.1406	0.1326	1392.7	6.93
60.0	45.0	0.2787	0.5273	0.0981	0.1456	0.1246	1386.8	9.67
60.0	60.0	0.1719	0.3475	0.0605	0.0851	0.0755	1403.4	11.41
60.0	75.0	0.0934	0.1537	0.0382	0.0458	0.0464	1414.7	9.27
60.0	90.0	0.0646	0.0426	0.0209	0.0250	0.0277	1420.7	-0.00
75.0	0.0	0.4458	0.4990	0.0513	0.0826	0.0833	1065.2	2.54
75.0	15.0	0.3790	0.6253	0.0458	0.0880	0.0775	1063.3	13.92
75.0	30.0	0.2929	0.6548	0.0290	0.0627	0.0516	1074.7	24.15
75.0	45.0	0.2014	0.6061	0.0136	0.0345	0.0249	1090.7	36.66
75.0	60.0	0.1331	0.5112	0.0040	0.0090	0.0088	1105.1	*****
75.0	75.0	0.0889	0.4313	0.0011	0.0041	0.0032	1113.1	-0.00
75.0	90.0	0.0803	0.3987	0.0035	0.0114	0.0076	1121.1	0.40
90.0	0.0	0.4492	0.6793	0.0662	0.1179	0.1064	1025.0	15.34
90.0	15.0	0.4426	0.6798	0.0627	0.1130	0.1016	1027.0	30.09
90.0	30.0	0.4193	0.7651	0.0815	0.1391	0.1204	990.1	44.93
90.0	45.0	0.4160	0.7544	0.0753	0.1309	0.1133	993.5	*****
90.0	60.0	0.4044	0.7705	0.0765	0.1319	0.1132	990.5	*****
90.0	75.0	0.4098	0.7449	0.0693	0.1168	0.1025	999.0	*****
90.0	90.0	0.4090	0.7406	0.0675	0.1135	0.1000	999.6	0.28

the constant RK and the elevation bias error θ_e. Thus the class of the object, or the aircraft type in our present case, obtained from η' does the required identification. We define a new term certainty of identification as

$$CER = D_2/(D_1 + D_2) \qquad (4-1)$$

where

D_1 = distance of unknown pattern vector from its nearest neighbor of the class identified

D_2 = distance of unknown pattern vector from its nearest neighbor of the other class.

4.7.2 Estimation of the Translational and Rotational Parameters

Information about the azimuth and roll angles, the constant RK and the elevation bias error θ_e is obtained from η', and is used to estimate the six parameters.

The values of the azimuth and roll angles obtained from η' are only approximate estimates for the two angles. A technique using linear interpolation is then used to generate 102 new pattern vectors of some known azimuth and roll angles around the nearest neighbor (ρ', η'). Let ψ_E and ϕ_E be the azimuth and roll angles obtained from η'. The closest 8 neighbors of $\vec{\rho}'$ from the sample set are the pattern vectors with the azimuth and roll angles as shown below in Figure 4.4. Using these 8 neighbors of $\vec{\rho}'$, we can generate 102 new pattern vectors for
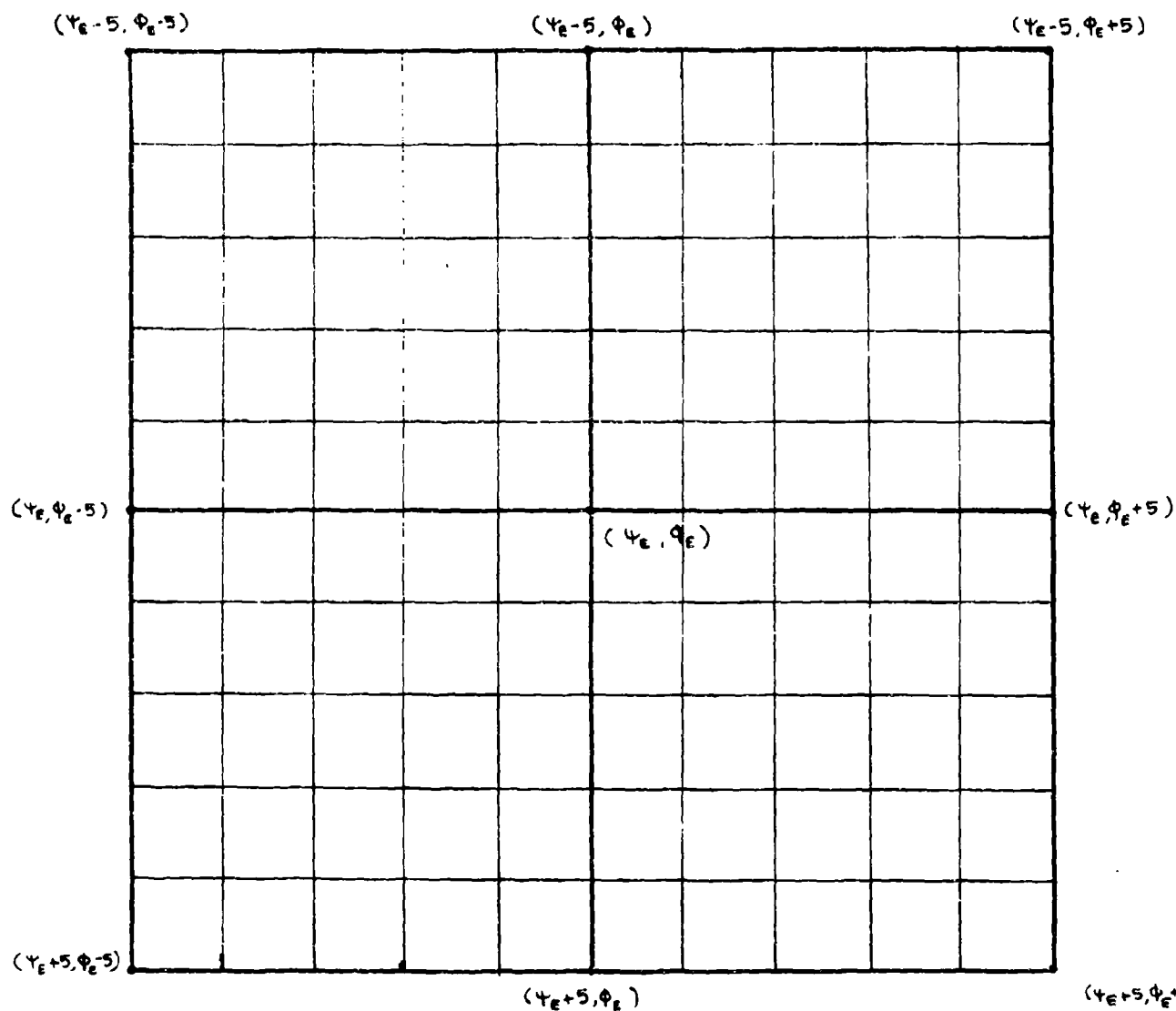
Figure 4.4   Values of ψ and ϕ for New Pattern
Vectors Generated by Interpolations

the variation in steps of 1 degree each in the values of the azimuth and roll angles. This is accomplished by interpolating the values of c_1, c_2, c_3, c_4 and c_5 separately for all the new positions shown in Figure 4.3 by using the above mentioned 8 neighbors. This is done by the INTP subroutine. The Nearest Neighbor Rule is then used again to find the closest match for the unknown vector $\vec{o}$ from the newly generated pattern vectors. Thus from this closest match found, we extract estimates for the azimuth and roll angles accurate up to 1 degree in noiseless cases.

The estimate for the distance of the unknown object along the optical axis is as shown below:

$$R_E = RK_E/r \qquad (4-2)$$

where RK_E is the value of the constant RK obtained from n', and r is the radius of gyration of the silhouette of the unknown object to be identified.

The inclination θ_m of the major axis of the ellipse fitted to the pattern can be found from Eq. (3-28), which appears below

$$\tan 2\theta_m = -2u_{11}/(u_{20} - u_{02})$$

and,

$$u_{20}' > u_{02}' \ . \qquad (4-3)$$

The elevation bias error θ_e for the unknown pattern vector is obtained from n', and therefore the estimate θ_E for the elevation angle is given by

$$\theta_E = \theta_m + \theta_e \qquad (4-4)$$

For the purpose of estimating the values of the off-axis distances A and C, we assume that the center of gravity of the unknown object is projected very near the centroid of its silhouette in the image plane. Therefore, from Eqs. (3-1) and (3-2), we have,

$$A_E = X_{CG} = U_{CG} \cdot (B_E + f)/f \qquad (4-5)$$

$$C_E = Y_{CG} = V_{CG} \cdot (B_E + f)/f \qquad (4-6)$$

where (U_{CG}, V_{CG}) is the centroid of the silhouette, B_E is the estimate for the distance along the optical axis and f is the focal length of the optical system. Thus we have been able to estimate the three translational and the three rotational parameters of the unknown object.

4.7.3 Results of Identification and Estimation in the Absence of Noise

Several silhouettes were generated with known reference translational and rotational parameters, and the pattern vector $\vec{\rho} = (\rho_1, \rho_2, \rho_3, \rho_4, \rho_5)$ was computed for each of the silhouettes. With the help of these pattern vectors, the identification and estimation was achieved.

Results of some of the identifications and estimations appear in Table XII.

It is seen from the results of Table XII, that the accuracy of the estimation of parameters is as shown below in Table XIII.

TABLE 13

ACCURACY OF ESTIMATION OF THE PARAMETERS

Parameters	Accuracy
Azimuth Angle	±1 degree
Roll Angle	±1 degree
Elevation Angle	±0.1 degree
Distance B	2 percent
Distance A	±2.0 feet
Distance C	±2.0 feet

It is to be noted from Table XII that the certainty of identification was always found to be very high, and from this we can infer that the clusters formed by the pattern vectors of each aircraft are nonoverlapping or separate.

4.7.4   Results of Identification and Estimation
         in the Presence of Noise

In a realistic system one would expect that the measurement points would not exactly overlay the boundary of the pattern from which they came. This error may be due to several different reasons. For instance, if the field of view has been slightly clouded over, or defocused, then the boundary of the pattern is no longer precise and the exact coordinates of points lying on the boundary can only be estimated. Even if the field of view is clear there is still the

TABLE 12

IDENTIFICATION AND ESTIMATION IN THE ABSENCE OF NOISE

	Type of Aircraft	A	C (in feet)	B	ψ	φ (in degrees)	θ	CER
1a. Reference Parameters	Phantom	2.0	1.0	6750	25	1	60.0	-
1b. Estimated Parameters	Phantom	1.5	0.5	6737	25	0	60.1	95
2a. Reference Parameters	Mirage	10.0	8.0	7525	13	18	12.0	-
2b. Estimated Parameters	Mirage	9.8	6.7	7828	13	17	12.1	98
3a. Reference Parameters	Mirage	8.0	0	9000	47	22	-41.0	-
3b. Estimated Parameters	Mirage	8.2	-0.5	8941	46	21	-41.0	100
4a. Reference Parameters	Phantom	0	2.0	10000	7	14	0.0	-
4b. Estimated Parameters	Phantom	-0.5	1.8	9841	6	15	0	99
5a. Reference Parameters	Mirage	1.0	10.0	5500	60	41	31.0	-
5b. Estimated Parameters	Mirage	2.2	9.8	5427	58	42	31.1	100
6a. Reference Parameters	Phantom	0	0	7000	22	3	-12.0	-
6b. Estimated Parameters	Phantom	-0.5	-0.5	7000	22	3	-12.0	100

possibility that the electronic equipment associated with the optical system can commit errors, be they internal or transmission errors. Furthermore, there is always the quantization error associated with analog to digital conversion. All of these errors may be considered as forms of noise.

A simulated silhouette for certain reference parameters for the Mirage appears in Figure 4.5 with a certain amount of noise added to the data points. The identification and estimation for this simulated silhouette is shown below in Table XIV.

TABLE 14

IDENTIFICATION AND ESTIMATION IN THE PRESENCE OF NOISE
(Aircraft Considered: Mirage, Aircraft was Identified to be Mirage)

Parameters	Reference Value	Estimated Value
Noise	3.4%	--
A	8.0 feet	7.7 feet
C	12.0 feet	12.0 feet
B	5500 feet	5496 feet
ψ	3°	0°
ϕ	13°	14°
θ	-40.0°	-40.1°
CER	--	100%

74
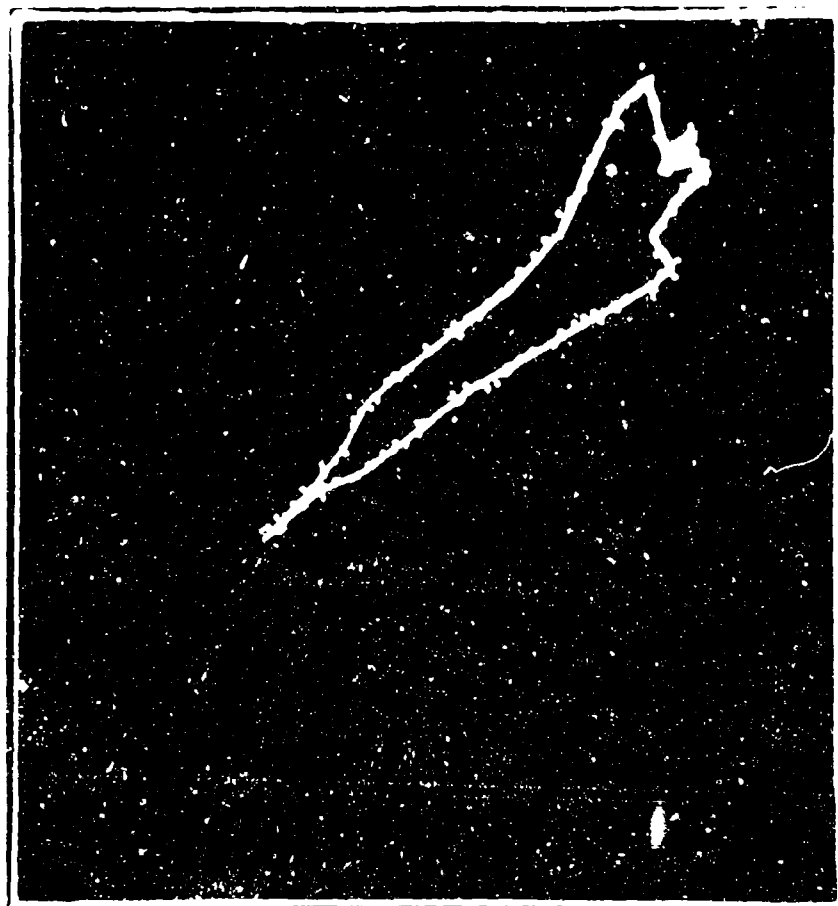
Figure 4.5 Perspective View of Mirage with A = 8 ft.,
B = 5550 ft., C = 12 ft., ψ = 3°, ϕ = 13°, 6 = -40.0°,
and with a noise of 3.4% added to the data points

Simulated silhouettes for certain reference parameters for the Phantom aircraft with different amounts of noise added appear in Figure 4.6 through 4.10. The identification and estimation for all these simulated silhouettes appear in Table 15. It should again be noted that the identification of the aircraft type was done correctly even in the presence of noise, and therefore showing the presence of nonoverlapping clusters formed by the pattern vectors of each aircraft.

Figure 4.6 Perspective View of Phantom with A = 10 ft.,
B = 7500 ft., C = 12 ft., ψ = 7°, ϕ = 22°, θ = 18°, and
with a noise of 0.0% added to the data points
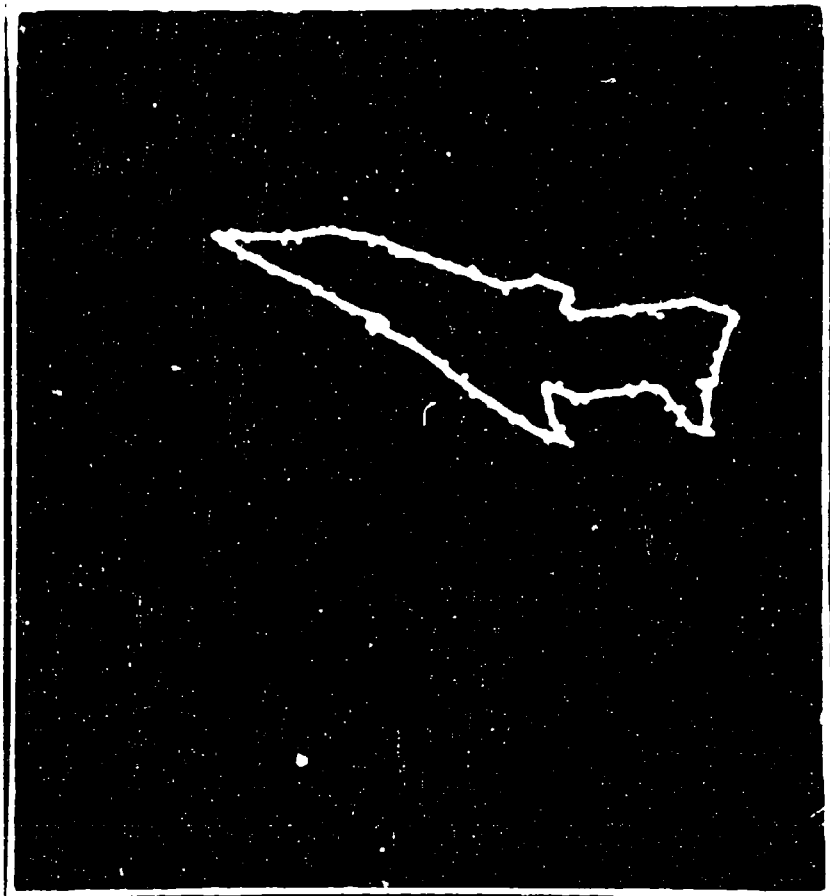
Figure 4.7 Perspective View of Phantom with A ≈ 10 ft.,
B = 7500 ft., C = 12 ft., ψ = 7°, ϕ = 22°, θ = 18°, and
with a noise of 2.2% added to the data points
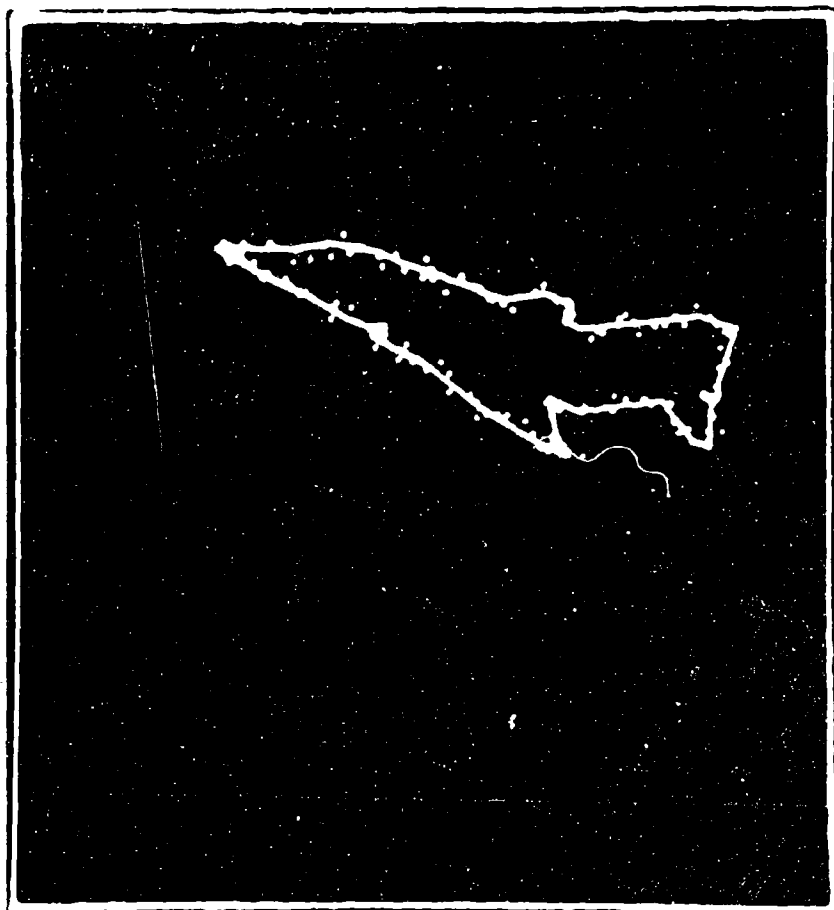
Figure 4.8 Perspective View of Phantom with A = 10 ft., B = 7500 ft., C = 12 ft., ψ = 7°, ϕ = 22°, θ = 18°, and with a noise of 4.8% added to the data points
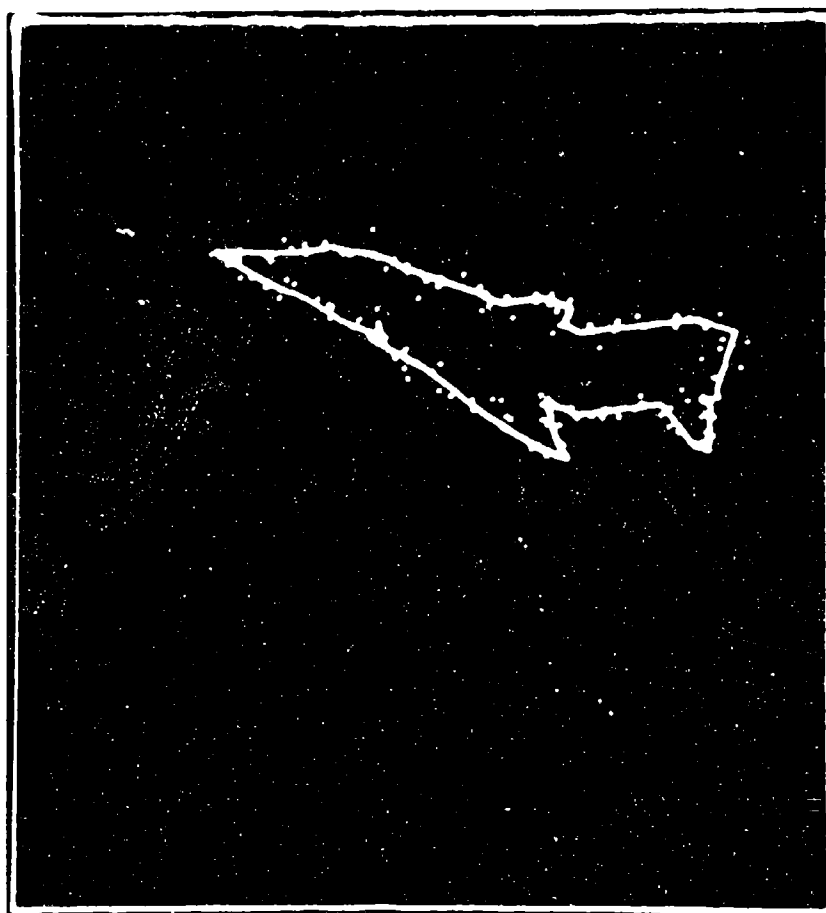
Figure 4.9 Perspective View of Phantom with A = 10 fc.,
B = 7500 ft., C = 12 ft., ψ = 7°, φ = 22°, θ = 18°, and
with a noise of 7.6% added to the data points
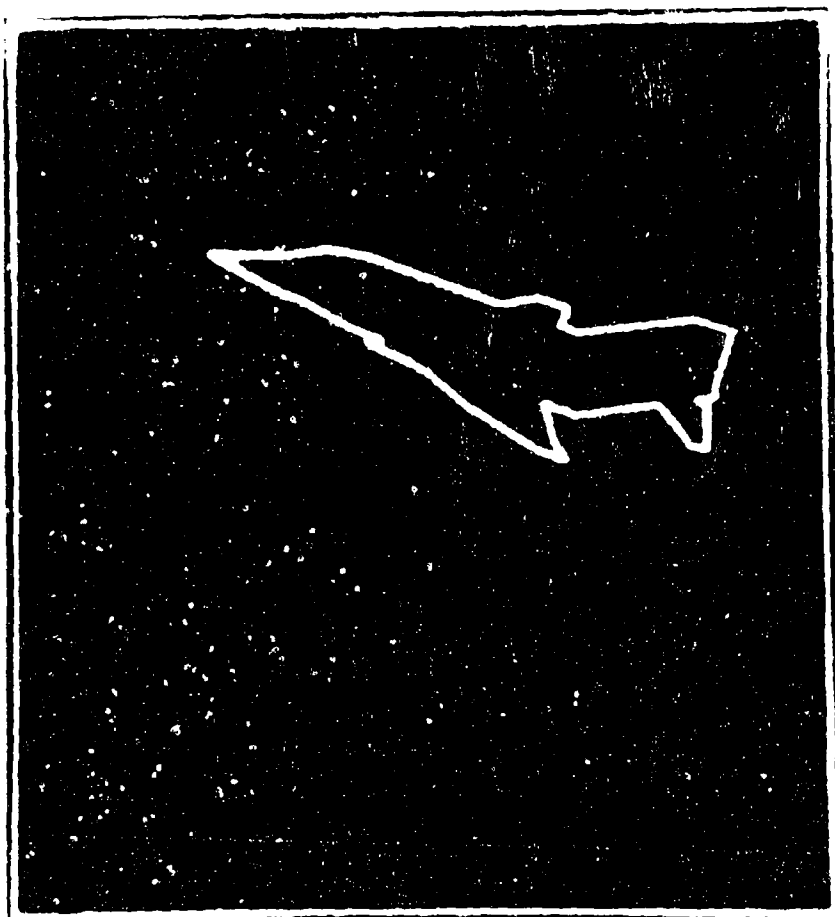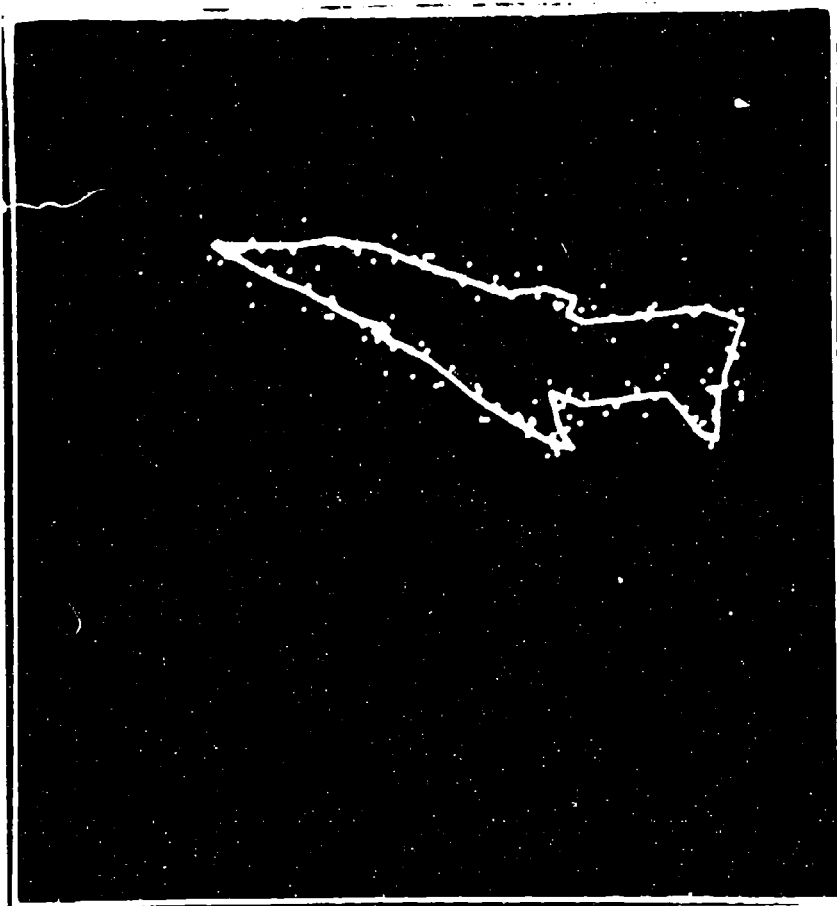
Figure 4.10 Perspective View of Phantom with A = 10 ft.,
B = 7500 ft., C = 12 ft., ψ = 7°, ϕ = 22°, θ = 18°, and
with a noise of 10.0% added to the data points

TABLE 15

IDENTIFICATION AND ESTIMATION IN THE PRESENCE OF NOISE
AIRCRAFT CONSIDERED: PHANTOM
REFERENCE PARAMETERS: A = 10 FEET, B = 7500 FEET, C = 12 FEET,
ψ = 7°, ϕ = 22°, θ = 18°
(Aircraft was always identified to be Phantom)

| Noise | Estimated Parameters | | | | | | |
	A	B	C	ψ	ϕ	θ	CER
0.0%	8.6	7468	12.3	8	22	18.1	77.8
2.2%	8.5	7459	22.0	7	22	18.1	82.8
4.8%	8.6	7512	12.4	5	23	18.3	86.4
7.6%	8.6	7474	12.4	7	22	18.1	81.9
10.0%	8.7	7479	12.3	2	24	18.2	94.6

CHAPTER V

SUMMARY AND CONCLUSIONS

This thesis is aimed at a solution to the problem of real time identification of three dimensional objects from their optical images. The approach taken here relies upon the invariant functions of moments which are used for the construction of the sample set.

The method of moments appears to work quite well for the identification of aircraft from their optical images. The results obtained in Chapter IV show that the performance of the method of moments for aircraft identification is comparable to that of a human photo interpreter, and it is roughly equivalent to or better than heuristic techniques. Failure to surpass the performance o. a human is not always a serious liability, however. In many situations, automation is required, even if the resulting performance is not as good as that of a human. When automation is required, the method of moments is quite possibly the best method, because it is easier to implement than the other heuristic techniques, which require point-by-point image analysis.

So far as is known to the author, no alternative image processing technique exists with a capability of real time identification and estimation of parameters of three dimensional objects. The algorithm developed in this research has the potential of reaching real time identification when a special purpose computer with multiprocessing

82

capabilities is used to do the requisite searches. An associative memory could also be used to store the sample set in order to decrease the identification time required.

While all of the results contained in this thesis relate to three different aircraft that were considered, it appears that this approach would be applicable for a larger number of objects as well. Further work in the following areas could lead to better accuracy in estimation of the parameters and in reduction of the limitations of the present method:

(1) An optimum distance function for use in the Nearest Neighbor Rule described in Chapter III.

(2) Linear separatibility for dividing the sample set into different regions or classes.

(3) Syntactic analysis to resolve the ambiguities between certain roll angles and azimuth angles such as between ϕ and $-\phi$, ψ and $-\psi$ or the nose and the tail of the aircraft.

(4) Design of a system to gather data, for use in moment calculations, from the optical image of an object.

```
      DIMENSION
 CC(6),CE(6),MCON(80,7),UD(3000),VD(3000),
    1 C1(6),C(6),P(80),Q(80),R(80)
      DIMENSION UBND(60),VBND(60)
      DIMENSION RM6(1,1),RK(1,1),
    1 RM1(1,1),RM2(1,1),RM3(1,1),RM4(1,1),RM5(1,1),
    1 EB(1,1)
      READ(6,1001) F,RPAT,UVLE,NPAR,NOP
1001  FORMAT(F6.1,F10.2,F5.1,2I3)
      READ(6,1002) (P(I),Q(I),R(I),I=1,NOP)
1002  FORMAT(3F9.4)
      READ(6,1003) CO(1),CO(2),CO(3)
1003  FORMAT(3F7.1)
      READ(6,1006) ((MCON(I,I1),I1=1,7),I=1,NOP)
1006  FORMAT(7I3)
      CALL RELEAS (6)
      F=12.
      UVLE=0.0002
      TYPE 600
600   FORMAT(' PLEASE TYPE DEC TAPE NO. IN FORMAT I1 ')
      READ(5,8886) IU
8886  FORMAT(I1)
      IU=IU+8
      TYPE 2211
2211  FORMAT('  ENTER AIRCRAFT CODE ')
      READ(5,2213) PLANE
2213  FORMAT(F2.0)
      TYPE 603
603   FORMAT(' ENTER CO-ORDINATES X,ZY IN FORMAT
2(F5.1,1X)
    1 .F8.1')
      READ(5,604) CO(1),CO(3),CO(2)
604   FORMAT(2(F5.1,1X),F8.1)
      TYPE 601
601   FORMAT(' ENTER ROLL,ASYMTH  ELEVATION ANGLES IN
FORMAT
      13(F5.1,1X) ')
      READ(5,602) CO(4),CO(5),CO(6)
602   FORMAT(3(F5.1,1X))
      TYPE 605
605   FORMAT(' ENTER SD IN FORMAT F6.4 ')
      READ(5,606) SD
606   FORMAT(F6.4)
      TYPE 1245
      READ(5,2468) IFN
2468  FORMAT(A3)
1245  FORMAT(' ENTER FILE NAME AS *** ',/)
      CALL OFILE(IU,IFN)
      WRITE(IU,4419) PLANE
4419  FORMAT(E15.7)
```

```
      WRITE(IU,4419) F
      WRITE(IU,4420) (CO(I),I=1,6)
4420  FORMAT(6E15.7)
      CO(6)=CO(6)+180.
      CALL RELEAS (5)
      DO 2025 I=1,NOP
      P(I)=P(I)*0.72
      Q(I)=Q(I)*0.72
      R(I)=R(I)*0.72
2025  CONTINUE
      XSUM=0.
      YSUM=0.
      ZSUM=0.
      DO 20 I=1,NOP
      XSUM=XSUM+P(I)
      YSUM=YSUM+Q(I)
      ZSUM=ZSUM+R(I)
20    CONTINUE
      DO 21 I=1,NOP
      P(I)=P(I)-(XSUM/NOP)
      Q(I)=Q(I)-(YSUM/NOP)
      R(I)=R(I)-(ZSUM/NOP)
21    CONTINUE
95    IA=1
510   IB=1
      CALL DATA(CO,P,Q,R,F,NOP,NPAR,HCON,UVLE,UD,
     1 VD,ISP1,SD,AM,SPAT,KM,UBND,VBND,ANOSE)
      TYPE 735,ISP1
735   FORMAT(' ISP1= ',I5)
      WRITE(IU,712) ANOSE
712   FORMAT(E15.7)
      WRITE(IU,716) KM
716   FORMAT(I5)
      WRITE(IU,720) (UBND(I),VBND(I),I=1,KM)
720   FORMAT(2E15.7)
      USUM=0.
      VSUM=0.
      DO 10 I=1,ISP1
      USUM=USUM+UD(I)
10    VSUM=VSUM+VD(I)
      UCG=USUM/ISP1
      VCG=VSUM/ISP1
      WRITE(IU,782) UCG,VCG
782   FORMAT(2E15.7)
      DO 11 I=1,ISP1
      UD(I)=UD(I)-UCG
11    VD(I)=VD(I)-VCG
      U20=0.
      UU2=0.
      U30=0.
```

```
      U11=0.
      U03=0.
      U12=0.
      U21=0.
      DO 80 I=1,ISP1
      U20=U20+UD(I)**2.
      U02=U02+VD(I)**2.
      U12=U12+UD(I)*VD(I)*VD(I)
      U21=U21+UD(I)*UD(I)*VD(I)
      U11=U11+UD(I)*VD(I)
      U03=U03+VD(I)**3.
 80   U30=U30+UD(I)**3.
      U02=U02/ISP1
      U20=U20/ISP1
      U30=U30/ISP1
      U11=U11/ISP1
      U21=U21/ISP1
      U12=U12/ISP1
      U03=U03/ISP1
      RM1(IA,IB)=U20+U02
      RG=SQRT(RM1(IA,IB))
      RM2(IA,IB)=(U20-U02)**2.+4.*U11*U11
      RM2(IA,IB)=RM2(IA,IB)/(RG**4.)
      RM3(IA,IB)=(U30-3.*U12)**2.+(3.*U21-U03)**2.
      RM3(IA,IB)=(RM3(IA,IB)**(4./6.))/(RG**4.)
      RM4(IA,IB)=(U30+U12)**2.+(U21+U03)**2.
      RM4(IA,IB)=(RM4(IA,IB)**(4./6.))/(RG**4.)
      RM5(IA,IB)=(U30-3.*U12)*(U30+U12)*((U30+U12)**2.
     1 -3.*(U21+U03)**2.)+(3.*U21-U03)*(U21+U03)*
     1 (3.*(U30+U12)**2.-(U21+U03)**2.)
      RM5(IA,IB)=(RM5(IA,IB)**(4./12.))/(RG**4.)
      RM6(IA,IB)=(U20-U02)*((U30+U12)**2.-(U21+U03)**2.)
     1 +4.*U11*(U30+U12)*(U21+U03)
      RM6(IA,IB)=(RM6(IA,IB)**(4./8.))/(RG**4.)
      U=(2.*U11)/(U02-U20)
      EB(IA,IB)=ATAN(U)
      EB(IA,IB)=90.*EB(IA,IB)/3.14
      CO6=EB(IA,IB)
      U20P=0.
      U02P=0.
      DO 1264 I=1,ISP1
      UDD=UD(I)*COSD(CO6)-VD(I)*SIND(CO6)
      VDD=UD(I)*SIND(CO6)+VD(I)*COSD(CO6)
      U20P=U20P+UDD**2.
      U02P=U02P+VDD**2.
1264  CONTINUE
      IF (U20P.GE.U02P) GO TO 1276
      IF (CO6.GT.0.) GO TO 1278
      CO6=CO6+90.
      GO TO 1276
```

```
1278 C06=C06-90.
1276 C06=C06
     DRT=ISP1/150.+1.
     ISPIN=INT(DRT)
     IMX=0
     DO 1300 I=1,ISP1,ISPIN
     IMX=IMX+1
1300 CONTINUE
     WRITE(IU,1307) IMX
     DO 1562 I=1,ISP1,ISPIN
     UD(I)=UD(I)+UCG
     VD(I)=VD(I)+VCG
     WRITE(IU,1308) JD(I),VD(I)
1562 CONTINUE
1308 FORMAT(2E15.7)
1307 FORMAT(I5)
     X1=RM2(IA,IB)
     X2=RM3(IA,IB)
     X3=RM4(IA,IB)
     X4=RM5(IA,IB)
     X5=RM6(IA,IB)
     WRITE(IU,1298) X1,X2,X3,X4,X5
1298 FORMAT(5E15.7)
     WRITE(IU,1098) C06,RG
1098 FORMAT(2E15.7)
     TYPE 1198,X1,X2,X3,X4,X5
1198 FORMAT(5(2X,F7.4))
     TYPE 1398,C06,RG
1398 FORMAT(2X,F5.1,4X,F6.4)
864  CALL RELEAS(IU)
     STOP
     END


     SUBROUTINE DATA(C,P,Q,R,F,NCP,NPAR,MCON,UVLE,UD,
    1 VD,ISP1,SD,AM,SPAT,KM,UBND,VBND,ANOSE)
     DIMENSION
C(6),P(80),MCON(80,7),UBND(60),VBND(60),
    1 UD(3000),VD(3000),IPN(50),Q(80),R(80)
     COMMON KMM,IUB(60),IVB(60)
     CALL PRDT(C,P,Q,R,F,NOP,NPAR,MCON,UBND,
    1 VBND,KM)
     DO 7 I=1,KM
     UB=(UBND(I+1)-UBND(I))**2.
     VB=(VBND(I+1)-VBND(I))**2.
     DST1=SQRT(UB+VB)
     PN=DST1/UVLE
     IPN(I)=INT(PN)
     PQ=PN-IPN(I)
     IF(PQ.LT.0.5) GO TO 1
```

```
      IPN(I)=IPN(I)+1
1     IF(IPN(I).NE.0) GO TO 2
      IPN(I)=1
2     DU=(UBND(I+1)-UBND(I))/IPN(I)
      DV=(VBND(I+1)-VBND(I))/IPN(I)
      IF(I.EQ.1) GO TO 4
      ISP=0
      DO 3 II=1,I-1
3     ISP=ISP+IPN(II)
      GO TO 5
4     ISP=0
5     IPN1=IPN(I)
      DO 6 II=1,IPN1
      IA=ISP+II
      UD(IA)=UBND(I)+(II-1)*DU
6     VD(IA)=VBND(I)+(II-1)*DV
7     CONTINUE
      ISP1=0
      DO 8 I=1,KM
      ISP1=ISP1+IPN(I)
8     CONTINUE
      ALNMX=-100.
      ALNMN=100.
      VZMAX=-100.
      DO 1752 I=1,KM
      IF (ALNMX.GE.UBND(I)) GO TO 1755
      ALNMX=UBND(I)
1755  IF (ALNMN.LE.UBND(I)) GO TO 1752
      ALNMN=UBND(I)
1752  CONTINUE
      AL1=ALNMX-ALNMN
      ALNMX=-100.
      ALNMN=100.
      DO 1758 I=1,KM
      IF (ALNMX.GE.VBND(I)) GO TO 1759
      ALNMX=VBND(I)
1759  IF (ALNMN.LE.VBND(I)) GO TO 1758
      ALNMN=VBND(I)
1758  CONTINUE
      AL2=ALNMX-ALNMN
      TYPE 1751,AL1,AL2
1751  FORMAT(2F6.4)
      AL=(AL1+AL2)/2.
      AM=0.
      DO 2147 I=1,ISP1
      CALL GAUSS(SD,AM,VZ,SPAT)
      UD(I)=UD(I)+VZ
      IF (VZMZX.GE.VZ) GO TO 2147
      VZMAX=VZ
2147  CONTINUE
```

```
      DO 2154 I=1,ISP1
      CALL GAUSS(SO,AM,VZ,SPAT)
      VO(I)=VO(I)+VZ
      IF (VZMAX.GE.VZ) GO TO 2154
      VZMAX=VZ
 2154 CONTINUE
      ANOSE=VZMAX*100./AL
      TYPE 1767,ANOSE
      TYPE 1767,VZMAX
 1767 FORMAT(F15.7)
      RETURN
      END




      SUBROUTINE PROT(D,P,Q,R,F,NOP,NPAR,MCON,UBND,
     1 VBND,KM)
      DIMENSION D(6),P(80),MCON(80,7),U(125),V(125),
     1 TA(500),TA1(500),UINT1(20),VINT1(20),UINT2(20),
     2 VINT2(20),L(20),LL(20),MKR(20),DII(20),DI(20),
     3 MKRKC(20),MKRII(20),UBND(60),VBND(60),TAO(60),
     4 MCON1(125,9),JKA(10),Q(80),R(80)
      D1=COSD(D(4))
      D2=SIND(D(4))
      D3=COSD(D(5))
      D4=SIND(D(5))
      D5=COSD(D(6))
      D6=SIND(D(6))
      D11=D5*D3
      D12=-D5*D4*D1+D6*D2
      D13=D5*D4*D2+D6*D1
      D21=D4
      D22=D3*D1
      D23=-D3*D2
      D31=-D6*D3
      D32=D6*D4*D1+D5*D2
      D33=-D6*D4*D2+D5*D1
      DO 41 I=1,NOP
      PX=P(I)*D11+Q(I)*D12+R(I)*D13+D(1)
      QY=P(I)*D21+Q(I)*D22+R(I)*D23+D(2)
      RZ=P(I)*D31+Q(I)*D32+R(I)*D33+D(3)
      U(I)=F*PX/(F+QY)
      V(I)=F*RZ/(F+QY)
   41 CONTINUE
      UMAX=U(1)
      JK=1
      DO 1 I=2,NOP
      IF(UMAX.GE.U(I)) GO TO 1
```

```
        UMAX=U(I)
        JK=1
1       CONTINUE
        UBND(1)=U(JK)
        VBND(1)=V(JK)
        TAO(1)=3.1415
        K1=2
        N1=NOP
        JKO=0
        NOP1=NOP+1
        DO 60 I=1,NOP
        DO 60 'I=1,7
60      MCON1(I,II)=MCON(I,II)
        DO 61 I=NOP1,125
        DO 61 II=1,9
61      MCON1(I,II)=0
        DO 62 I=1,NOP
        DO 62 II=8,9
62      MCON1(I,II)=0
2       JN1=0
        DO 10 I=1,N1
        IF(I.EQ.JK.OR.I.EQ.JKO) GO TO 9
        DO 400 J=1,9
        IF(MCON1(JK,J).EQ.I) GO TO 401
400     CONTINUE
        GO TO 9
401     IF(U(I).EQ.U(JK)) GO TO 3
        XX=(V(I)-V(JK))/(U(I)-U(JK))
        TA(I)=ATAN(XX)
        IF(U(I).LT.U(JK)) GO TO 7
        IF(V(I).LT.V(JK)) GO TO 8
        GO TO 10
3       IF(V(I)-V(JK)) 4,5,6
4       TA(I)=4.7123
        GO TO 10
5       TA(I)=20.0
        JN1=JN1+1
        JKA(JN1)=I
        GO TO 10
6       TA(I)=1.5707
        GO TO 10
7       TA(I)=TA(I)+3.1415
        GO TO 10
8       TA(I)=TA(I)+6.2831
        GO TO 10
9       TA(I)=20.0
10      CONTINUE
        DO 13 I=1,N1
        TA1(I)=TA(I)-TAO(K1-1)+3.1415
        IF(TA1(I).LT.0.0) GO TO 11
```

```
      IF(TA1(I).GE.6.2831) GO TO 12
      GO TO 13
11    TA1(I)=TA1(I)+6.2831
      GO TO 13
12    TA1(I)=TA1(I)-6.2831
13    CONTINUE
      TAM=TA1(1)
      JN=1
      DO 14 I=2,N1
      IF(TAM.LE.TA1(I)) GO TO 14
      TAM=TA1(I)
      JN=1
14    CONTINUE
      TAO(K1)=TA(JN)
      N2=N1-1
      KCLM=0
      DO 26 I=1,N2
      KCL=0
      IF(I.EQ.JK.OR.I.EQ.JN) GO TO 26
      DO 24 II=2,N1
      IF(II.EQ.JK.OR.II.EQ.JN) GO TO 24
      IF(II.LE.I) GO TO 24
      DO 500 J=1,9
      IF(MCON1(I,J).EQ.II) GO TO 600
500   CONTINUE
      GO TO 24
600   A1=U(I)-U(II)
      A2=J(JN)-U(JK)
      B1=V(I)-V(II)
      B2=V(JN)-V(JK)
      AX=A1*B2-A2*B1
      ABSAX=ABS(AX)
      IF(ABSAX.LE.1.0E-6) GO TO 24
      A=((U(JN)-U(II))*B2-A2*(V(JN)-V(II)))/AX
      B=(A1*(V(JN)-V(II))-(U(JN)-U(II))*B1)/AX
      AL1=1.00000001
      AL2=0.99999999
      EPS1=-0.00000001
      EPS2=0.00000001
      IF(A.GT.AL1.OR.B.GT.AL1) GO TO 24
      IF(A.LT.EPS1.OR.B.LT.EPS1) GO TO 24
      IF(A.LE.EPS2.AND.A.GE.EPS1) GO TO 17
      IF(A.LE.AL1.AND.A.GE.AL2) GO TO 18
      GO TO 19
17    IF(B.GE.EPS1.AND.B.LE.EPS2) GO TO 24
      IF(B.GE.AL2.AND.B.LE.AL1) GO TO 24
      KCL=KCL+1
      L(KCL)=1
      UINT1(KCL)=U(II)
      VINT1(KCL)=V(II)
```

```
         GO TO 23
18       IF(B.GE.EPS1.AND.B.LE.EPS2) GO TO 24
         IF(B.GE.AL2.AND.B.LE.AL1) GO TO 24
         KCL=KCL+1
         L(KCL)=2
         UINT1(KCL)=J(I)
         VINT1(KCL)=V(I)
         GO TO 23
19       IF(B.GE.EPS1.AND.B.LE.EPS2) GO TO 20
         IF(B.GE.AL2.AND.B.LE.AL1) GO TO 21
         KCL=KCL+1
         L(KCL)=3
         UINT1(KCL)=A*J(I)+(1.-A)*U(II)
         VINT1(KCL)=A*V(I)+(1.-A)*V(II)
         GO TO 23
20       KCL=KCL+1
         L(KCL)=4
         UINT1(KCL)=U(JN)
         VINT1(KCL)=V(JN)
         GO TO 23
21       KCL=KCL+1
         L(KCL)=5
         UINT1(KCL)=U(JK)
         VINT1(KCL)=V(JK)
23       MKR(KCL)=II
         AA=U(JK)-UINT1(KCL)
         BB=V(JK)-VINT1(KCL)
         DII(KCL)=SQRT(AA**2.+BB**2.)
24       CONTINUE
         IF(KCL.EQ.0) GO TO 26
         KCLM=KCLM+1
         MKRKC(KCLM)=I
         DI(KCLM)=DII(1)
         J1=1
         IF(KCL.EQ.1) GO TO 50
         DO 25 III=2,KCL
         IF(DI(KCLM).LE.DII(III)) GO TO 25
         DI(KCLM)=DII(III)
         J1=III
25       CONTINUE
50       MKRII(KCLM)=MKR(J1)
         LL(KCLM)=L(J1)
         UINT2(KCLM)=UINT1(J1)
         VINT2(KCLM)=VINT1(J1)
26       CONTINUE
         IF(KCLM.EQ.0) GO TO 34
         DMN=DI(1)
         LPA=1
         IF(KCLM.EQ.1) GO TO 28
         DO 27 I=2,KCLM
```

```
              IF(DMN.LE.DI(I)) GO TO 27
              DMN=DI(I)
              LPA=I
      27      CONTINUE
      28      UBND(K1)=UINT2(LPA)
              VBND(K1)=VINT2(LPA)
              LI=MKRKC(LPA)
              LII=MKRII(LPA)
              DO 100 J=1,9
              IF(MCON1(LI,J).EQ.LII) GO TO 200
              GO TO 100
      200     JI1=J
              GO TO 300
      100     CONTINUE
      300     DO 101 J=1,9
              IF(MCON1(LII,J).EQ.LI) GO TO 201
              GO TO 101
      201     JI2=J
              GO TO 301
      101     CONTINUE
      301     DO 102 J=1,9
              IF(MCON1(JK,J).EQ.JN) GO TO 202
              GO TO 102
      202     JI3=J
              GO TO 302
      102     CONTINUE
      302     DO 103 J=1,9
              IF(MCON1(JN,J).EQ.JK) GO TO 203
              GO TO 103
      203     JI4=J
              GO TO 303
      103     CONTINUE
      303     IF(LL(LPA).EQ.1) GO TO 29
              IF(LL(LPA).EQ.2) GO TO 30
              IF(LL(LPA).EQ.3) GO TO 31
              IF(LL(LPA).EQ.4) GO TO 32
              MCON1(LI,JI1)=JK
              MCON1(LII,JI2)=JK
              MCON1(JK,8)=LI
              MCON1(JK,9)=LII
              GO TO 2
      29      MCON1(JK,JI3)=LII
              MCON1(JN,JI4)=LII
              MCON1(LII,8)=JK
              MCON1(LII,9)=JN
              JKO=JK
              JK=LII
              GO TO 33
      30      MCON1(JK,JI3)=LI
              MCON1(JN,JI4)=LI
```

```
        MCON1(L1,8)=JK
        MCON1(L1,9)=JN
        JKD=JK
        JK=L1
        GO TO 33
31      N1=N1+1
        MCON1(JK,JI3)=N1
        MCON1(JN,J14)=N1
        MCON1(L1,J11)=N1
        MCON1(L11,J12)=N1
        MCON1(N1,1)=L1
        MCON1(N1,2)=L11
        MCON1(N1,3)=JK
        MCON1(N1,4)=JN
        MCON1(N1,5)=0
        MCON1(N1,6)=0
        MCON1(N1,7)=0
        U(N1)=UBND(K1)
        V(N1)=VBND(K1)
        JKD=JK
        JK=N1
        GO TO 33
32      MCON1(L1,J11)=JN
        MCON1(L11,J12)=JN
        MCON1(JN,8)=L1
        MCON1(JN,9)=L11
        JKD=JK
        JK=JN
33      K1=K1+1
        GO TO 2
34      IF(U(JN).EQ.UBND(1).AND.V(JN).EQ.VBND(1))
       1 GO TO 35
        UBND(K1)=U(JN)
        VBND(K1)=V(JN)
        JKD=JK
        JK=JN
        K1=K1+1
        GO TO 2
35      KM=K1-1
        UBND(KM+1)=UBND(1)
        VBND(KM+1)=VBND(1)
        RETURN
        END



        SUBROUTINE GAUSS(SD,AM,VZ,SPAT)
        A=0.
        DO 50 KAA=1,12
```

```
              Y=RAN(SPAT)
     50       A=A+Y
              VZ=(A-6.)*SD+AM
              RETURN
              END




              DIMENSION
     X11(19,19),X12(19,19),X13(19,19),X14(19,19),
            1 X15(19,19),RK1(19,19),EB1(19,19)
              DIMENSION
     X21(19,19),X22(19,19),X23(19,19),X24(19,19),
            1 X25(19,19),RK2(19,19),EB2(19,19)
              DIMENSION X1(11,11),X2(11,11),X3(11,11),
            1 X4(11,11),X5(11,11)
              DIMENSION CO(6)
              DIMENSION UD(220),VD(220),UBND(60),VBND(60)
              TYPE 100
     100      FORMAT(' ENTER ) C TAPE NO. ')
              READ(5,120) IU
     120      FORMAT(I1)
              IU=IU+8
              IF (IU.NE.17) GO TO 140
              TYPE 150
     150      FORMAT('  LOADING OF MONENT TABLES ')
              TYPE 170
     170      FORMAT(' ENTER DEC TAPE NO. ')
              READ(5,190) IU
     190      FORMAT(I1)
              IU=IU+8
              CALL IFILE(IU,'PHAN')
              DO 610 I=1,19
              DO 611 II=1,19
              READ(IU,250) AZ,RO,X11(I,II),X12(I,II),X13(I,II),
            1 X14(I,II),X15(I,II),RK1(I,II),EB1(I,II)
     611      CONTINUE
     610      CONTINUE
              CALL RELEAS (IU)
              CALL IFILE(IU,'MIR')
              DO 310 I=1,19
              DO 311 II=1,19
              READ(IU,250) AZ,RO,X21(I,II),X22(I,II),X23(I,II),
            1 X24(I,II),X25(I,II),RK2(I,II),EB2(I,II)
     311      CONTINUE
     310      CONTINUE
              CALL RELEAS (IU)
     250      FORMAT(2F6.1,7E15.7)
```

```
        TYPE 390
390     FORMAT(' END OF LOADING ')
        READ(5,250) END
140     IF (IU.EQ.8) GO TO 420
        TYPE 430
430     FORMAT(' ENTER FILE NAME AS *** ',/)
        READ(5,450) IFN
450     FORMAT(A3)
        CALL IFILE(IU,IFN)
        READ(IU,480) PLANE
480     FORMAT(E15.7)
        READ(IU,480) F
        READ(IU,500) (CO(I),I=1,6)
500     FORMAT(6E15.7)
        READ(IU,480) ANOSE
        READ(IU,530) KM
530     FORMAT(I5)
        READ(IU,550) (UBND(I),VBND(I),I=1,KM)
550     FORMAT(2E15.7)
        READ(IU,550) UCG,VCG
        READ(IU,530) ISP1
        READ(IU,550) (UD(I),VD(I),I=1,ISP1)
        READ(IU,600) Y1,Y2,Y3,Y4,Y5
600     FORMAT(5E15.7)
        READ(IU,550) CO6,RG
        CALL RELEAS (IU)
420     DM1=1000.
        DM2=1000.
        TYPE 635,ANOSE
635     FORMAT(' NOISE= ',F6.1)
        TYPE 637,PLANE
637     FORMAT(' AIRCRAFT CODE= ',F3.1)
        CO(1)=CO(1)/12.
        CO(3)=CO(3)/12.
        CO(2)=CO(2)/12.
        TYPE 1190,CO(1),CO(3)
        TYPE 1210,CO(2)
        TYPE 1230,CO(4),CO(5),CO(6)
        CALL DIS(UBND,VBND,KM,UD,VD,ISP1)
        DO 640 I=1,19
        DO 650 II=1,19
        DR1=(Y1-X11(I,II))**2.+(Y2-X12(I,II))**2.
     1  +(Y3-X13(I,II))**2.+(Y4-X14(I,II))**2.
     1  +(Y5-X15(I,II))**2.
        IF (DM1.LE.DR1) GO TO 690
        DM1=DR1
        IA1=I
        IR1=II
690     DR2=(Y1-X21(I,II))**2.+(Y2-X22(I,II))**2.
     1  +(Y3-X23(I,II))**2.+(Y4-X24(I,II))**2.
```

```
      1 +(Y5-X25(I,II))**2.
      IF (DM2.LE.DR2) GO TO 650
      IA2=I
      IR2=II
      DM2=DR2
650   CONTINUE
640   CONTINUE
      IF (DM2.LE.DM1) GO TO 820
      CER=DM2/(DM2+DM1)
      PL=1.
      CO6=CO6-EB1(IA1,IR1)
      CO2=RK1(IA1,IR1)/RG
      CALL INTP(IA1,IR1,X11,X1)
      CALL INTP(IA1,IR1,X12,X2)
      CALL INTP(IA1,IR1,X13,X3)
      CALL INTP(IA1,IR1,X14,X4)
      CALL INTP(IA1,IR1,X15,X5)
      GO TO 915
820   CER=DM1/DM1+DM2
      PL=2.
      CO6=CO6-EB2(IA2,IR2)
      CO2=RK2(IA2,IR2)/RG
      CALL INTP(IA2,IR2,X21,X1)
      CALL INTP(IA2,IR2,X22,X2)
      CALL INTP(IA2,IR2,X23,X3)
      CALL INTP(IA2,IR2,X24,X4)
      CALL INTP(IA2,IR2,X25,X5)
915   CER=CER*100.
      DM=1000.
      DO 1010 I=1,11
      DO 1020 II=1,11
      D=(Y1-X1(I,II))**2.+(Y2-X2(I,II))**2.
      1 +(Y3-X3(I,II))**2.+(Y4-X4(I,II))**2.
      1 +(Y5-X5(I,II))**2.
      IF (DM.LE.D) GO TO 1020
      DM=D
      IAD=I
      IRD=II
1020  CONTINUE
1010  CONTINUE
      CO1=UCG*(F+CO2)/F
      CO3=VCG*(F+CO2)/F
      TYPE 1122
1122  FORMAT(' ESTIMATED VALUES ')
      IF (PL.NE.1.) GO TO 1130
      CO5=5.*(IA1-1.)+(IAD-6.)
      CO4=5.*(IR1-1.)+(IRD-6.)
      TYPE 1355,IA1,IR1,IAD,IRD
1355  FORMAT(4I10)
      TYPE 1152,CER
```

```
1152 FORMAT(' AIRCRAFT IDENTIFIED TC BE
PHANTCM,CERTAINTY=',
     1 F5.1)
     GO TC 1160
1130 CU5=5.*(IA2-1.)+(IAD-6.)
     CD4=5.*(IR2-1.)+(IRD-6.)
     TYPE 1355,IA2,IR2,IAD,IRD
     TYPE 1182,CER
1182 FORMAT(' AIRCRAFT IDENTIFIED TO BE
MIRAGE,CERTAINTY=',
     1 F5.1)
1160 CO1=CO1/12.
     CO3=CO3/12.
     CO2=CO2/12.
     TYPE 1190,CO1,CO3
1190 FORMAT(' X= ',F6.1,' Z= ',F6.1)
     TYPE 1210,CO2
1210 FORMAT('  Y=   ',F10.1)
     TYPE 1230,CO4,CO5,CO6
1230 FORMAT(' ROLL ANG.= ',F5.1,' AZIMJTH ANG.= ',
     1 F5.1,' ELEVATION ANG.= ',F5.1)
     STOP
     END




     SUBROUTINE INTP(IA,IR,XX,T)
     DIMENSION XX(19,19),T(11,11)
     A5=XX(IA,IR)
     IF (IA.EQ.1) GO TU 30
     A2=XX(IA-1,IR)
     IF (IR.NE.1) GO TO 40
     A1=1000.
     A4=1000.
     A7=1000.
     A6=XX(IA,IR+1)
     A3=XX(IA-1,IR+1)
     GO TC 50
40   A1=XX(IA-1,IR-1)
     A4=XX(IA,IR-1)
     IF (IR.NE.19) GO TO 60
     A3=1000.
     A6=1000.
     A9=1000.
     GO TO 70
60   A3=XX(IA-1,IR+1)
     A6=XX(IA,IR+1)
```

```
      IF (IA.NE.19) GO TO 80
      A7=1000.
      A8=1000.
      A9=1000.
      GO TO 500
80    A7=XX(IA+1,IR-1)
      A8=XX(IA+1,IR)
      A9=XX(IA+1,IR+1)
      GO TO 500
50    IF (IA.NE.19) GO TO 100
      A8=1000.
      A9=1000.
      GO TO 500
100   A8=XX(IA+1,IR)
      A9=XX(IA+1,IR+1)
      GO TO 500
70    IF (IA.NE.19) GO TO 120
      A7=1000.
      A8=1000.
      GO TO 500
120   A7=XX(IA+1,IR-1)
      A8=XX(IA+1,IR)
      GO TO 500
30    A1=1000.
      A2=1000.
      A3=1000.
      A8=XX(IA+1,IR)
      IF (IR.NE.1) GO TO 200
      A4=1000.
      A7=1000.
      A6=XX(IA,IR+1)
      A9=XX(IA+1,IR+1)
      GO TO 500
200   IF (IR.NE 19) GO TO 300
      A6=1000.
      A9=1000.
      A4=XX(IA,IR-1)
      A7=XX(IA+1,IR-1)
      GO TO 500
300   A4=XX(IA,IR-1)
      A6=XX(IA,IR+1)
      A7=XX(IA+1,IR-1)
      A9=XX(IA+1,IR+1)
500   CALL EQPT(A1,A4,A7,T(1,1),T(2,1),T(3,1),T(4,1),
     1
     T(5,1),T(6,1),T(7,1),T(8,1),T(9,1),T(10,1),T(11,1))
      CALL
     EQPT(A3,A6,A9,T(1,11),T(2,11),T(3,11),T(4,11),
     1
     T(5,11),T(6,11),T(7,11),T(8,11),T(9,11),T(10,11),
```

```
      1 T(11,11))
        CALL
EQPT(A2,A5,A6,T(1,6),T(2,6),T(3,6),T(4,6),T(5,6),
      1 T(6,6),T(7,6),T(8,6),T(9,6),T(10,6),
      1 T(11,6))
        CALL EQPT(T(1,1),T(1,6),T(1,11),
      1 T(1,1),T(1,2),T(1,3),T(1,4),T(1,5),
      1 T(1,6),T(1,7),T(1,8),T(1,9),T(1,10),T(1,11))
        CALL EQPT(T(2,1),T(2,6),T(2,11),
      1 T(2,1),T(2,2),T(2,3),T(2,4),T(2,5),T(2,6),
      1 T(2,7),T(2,8),T(2,9),T(2,10),T(2,11))
        CALL EQPT(T(3,1),T(3,6),T(3,11),
      1 T(3,1),T(3,2),T(3,3),T(3,4),T(3,5),T(3,6),
      1 T(3,7),T(3,8),T(3,9),T(3,10),T(3,11))
        CALL EQPT(T(4,1),T(4,6),T(4,11),
      1 T(4,1),T(4,2),T(4,3),T(4,4),T(4,5),T(4,6),
      1 T(4,7),T(4,8),T(4,9),T(4,10),T(4,11))
        CALL EQPT(T(5,1),T(5,6),T(5,11),
      1 T(5,1),T(5,2),T(5,3),T(5,4),T(5,5),T(5,6),
      1 T(5,7),T(5,8),T(5,9),T(5,10),T(5,11))
        CALL EQPT(T(6,1),T(6,6),T(6,11),
      1 T(6,1),T(6,2),T(6,3),T(6,4),T(6,5),T(6,6),
      1 T(6,7),T(6,8),T(6,9),T(6,10),T(6,11))
        CALL EQPT(T(7,1),T(7,6),T(7,11),
      1 T(7,1),T(7,2),T(7,3),T(7,4),T(7,5),T(7,6),
      1 T(7,7),T(7,8),T(7,9),T(7,10),T(7,11))
        CALL EQPT(T(8,1),T(8,6),T(8,11),
      1 T(8,1),T(8,2),T(8,3),T(8,4),T(8,5),T(8,6),
      1 T(8,7),T(8,8),T(8,9),T(8,10),T(8,11))
        CALL EQPT(T(9,1),T(9,6),T(9,11),
      1 T(9,1),T(9,2),T(9,3),T(9,4),T(9,5),T(9,6),
      1 T(9,7),T(9,8),T(9,9),T(9,10),T(9,11))
        CALL EQPT(T(10,1),T(10,6),T(10,11),
      1
T(10,1),T(10,2),T(10,3),T(10,4),T(10,5),T(10,6),
      1 T(10,7),T(10,8),T(10,9),T(10,10),T(10,11))
        CALL EQPT(T(11,1),T(11,6),T(11,11),
      1
T(11,1),T(11,2),T(11,3),T(11,4),T(11,5),T(11,6),
      1 T(11,7),T(11,8),T(11,9),T(11,10),T(11,11))
        RETURN
        END




        SUBROUTINE EQPT(X1,X2,X3,Y1,Y2,Y3,Y4,Y5,Y6,Y7,Y8,
      1 Y9,Y10,Y11)
        D1=(X2-X1)/5.
```

```
      D2=(X3-X2)/5.
      Y1=X1
      Y2=Y1+D1
      Y3=Y2+D1
      Y4=Y3+D1
      Y5=Y4+D1
      Y6=X2
      Y7=Y6+D2
      Y8=Y7+D2
      Y9=Y8+D2
      Y10=Y9+D2
      Y11=X3
      RETURN
      END




      SUBROUTINE DIS(UBND,VBND,KM,UD,VD,ISP1)
      DIMENSION UBND(60),VBND(60)
      DIMENSION UD(250),VD(250)
      DIMENSION A(1000)
      UBND(KM+1)=UBND(1)
      VBND(KM+1)=VBND(1)
      CD=10000.
      COMMON LP,ISHOW,XMAX,XMIN,YMAX,YMIN,INTENS,
     1 ISCALE
      LP=0
      ISHOW=0
      INTENS=7
      ISCALE=0
      KMM=KM+1
13    DO 1 I=1,KMM
      UBND(I)=CD*UBND(I)+1000.
      VBND(I)=CD*VAND(I)+1000.
1     CONTINUE
      DO 65 I=1,ISP1
      UD(I)=CD*UD(I)+1000.
      VD(I)=CD*VD(I)+1000.
65    CONTINUE
11    CALL INTAB(A,1000)
      XMAX=2000.
      XMIN=0.
      YMAX=2000.
      YMIN=0.
      CALL POINT(A,UBND(1),VBND(1))
      ISHOW=1
      DO 2 I=1,KM
      CALL LINE(A,UBND(I),VBND(I),UBND(I+1),VBND(I+1))
```

```
2       CONTINUE
        CALL POINT(A,50.,50.)
        CALL LINE(A,50.,50.,1950.,50.)
        CALL LINE(A,1950.,50.,1950.,1950.)
        CALL LINE(A,1950.,1950.,50.,1950.)
        CALL LINE(A,50.,1950.,50.,50.)
        DO 35 I=1,ISP1
        CALL SPOT(A,UD(I),VD(I))
35      CONTINUE
        CALL DISPLY(1,A)
        TYPE 3
3       FORMAT(' TYPE MAG. FACTOR IN FORMAT F4.1 ')
        READ(5,7) AB
7       FORMAT(F4.1)
15      DO 66 I=1,ISP1
        UD(I)=(UD(I)-1000.)/CD
        VD(I)=(VD(I)-1000.)/CD
66      CONTINUE
        DO 3252 I=1,KMM
        UBND(I)=(UBND(I)-1000.)/CD
        VBND(I)=(VBND(I)-1000.)/CD
3252    CONTINUE
        CD=AB*CD
        IF (AB.NE.1.) GO TO 13
        RETURN
        END
```

REFERENCES

1. M.K. Hu, "Visual Pattern Recognition by Moment Invariants," IRE Trans. Information Theory, Vol. IT-8, pp. 179-187, February 1962.

2. I.E. Sutherland, "Computer Displays," Scientific American, pp. 57-81, June 1970.

3. J.H. Munson, "Some views on Pattern-recognition Methodology," Internatl. Conf. Methodologies of Pattern Recognition, University of Hawaii, Honolulu, January 24-26, 1968.

4. T. Kasvand, "Computer Simulation of Pattern Recognition by Using Cell-assemblies and Contour Projection," 1965 Proc. IFAC Tokyo Symp. Sys. Engrg. Control Sys. Design, pp. 203-210.

5. M.D. Levine, "Feature Extraction: A Survey," Proc. of the IEEE, Vol. 57, No. 8, pp. 1391-1407, August 1969.

6. O.G. Selfridge and U. Neisser, "Pattern Recognition and Modern Computers," Proc. Western Joint Computer Conf., pp. 91-93, March 1955.

7. H. Kazmierczak and K. Steinbuch, "Adaptive Systems in Pattern Recognition," IEEE Trans. Electronic Computers, Vol. EC-12, pp. 822-835, December 1963.

8. R.O. Duda, P.E. Hart, and J.M. Munson, "Graphical-data-processing Research Study and Experimental Investigation," Stanford Research Institute, Menlo Park, Calif., Tech. Rept. ECOM-01901-26, March 1967.

9. G.S. Sebestyen, "Machine Aided Reconnaissance Photointerpretation," 8th SPIE Tech. Symp., Los Angeles, Calif., August 1963.

10. D.G. Lebedev and D.S. Lebedev, "Quantizing the Images by Separation and Quantization of Contours," Engrg. Cybernetics, No. 1, pp. 77-81, January-February 1965.

11. S.H. Unger, "Pattern Detection and Recognition," Proc. IRE, Vol. 47, pp. 1737-1752, October 1959.

12. W. Sprick and K. Ganzhorn, "An Analogus Method for Pattern Recognition by Following the Boundary," Proc. Internatl. Conf. Information, Paris: UNESCO, pp. 238-244, June 15-20, 1959.

13. E.C. Greanias, P.F. Meagher, R.J. Norman, and P. Essinger, "The Recognition of Handwritten numerals by Contour Analysis," IBM J. Res. and Develop., Vol. 7, No. 1, pp. 14-21, January 1963.

14. H. Hemami, R.B. McGhee, and S.R. Gardner, "Towards a Generalized Template Matching Algorithm for Pictorial Pattern Recognition," Proceedings of the 1970 IEEE Symposium on Adaptive Processes, Austin, Texas, December 7-9, 1970.

15. T. Kasvand, "Recognition of Monochromatic Two-dimensional Objects," report available from the author at The National Research Council of Canada, Ottawa, Ontario, 1968.

16. K. Paton, "Conic Sections in Chromosome Analysis," Pattern Recognition, Pergamon Press 1970, Vol. 2, pp. 39-51, Great Britain.

17. H. Blum, "An Associative Machine for Dealing with the Visual Field and Some of its Biological Implications," Air Force Cambridge Research Laboratories, Bedford, Mass., Electronics Research Directorate, Rept. AFCRL62-62, February 1962.

18. H. Blum, "A Transformation for Extracting New Descriptors of Shape," Models for the Perception of Speech and Visual Form, Boston, Mass.: M.I.T. Press, 1967, pp. 362-380.

19. G.S. Sebestyen, "Pattern Recognition by an Adaptive Process of Sample Set Construction," Trans. IRE, IT-8, 5, September 1962.

20. R.A. Weiss, "BE VISION, A Package of IBM 7090 FORTRAN Programs to Draw Orthographic views of Combinations of Plane and Quadric Surfaces," Journal of ACM, Vol. 13, No.2, pp. 194-204, April 1966.

21. P.G. Comba, "A Procedure for Detecting Intersections of 3-D Objects," Journal of ACM, Vol. 15, No.3, pp. 354-366, July 1968.

22. P.P. Loutrel, "A Solution to the Hidden-Line Problem for Computer Drawn Polyhedra," IEEE Transactions on Computers, Vol. C-19, No. 3, pp. 205-213, March 1970.

23. A. Guzman, "Computer Recognition of Three-Dimensional Objects in a Visual Scene," Report MAC-TR-59 (Thesis), Cambridge, Mass.: Project MAC, MIT, December 1968.

24. P.H. Winston, "Learning Structural Descriptions from Examples,: Report MAC-TR-76, Cambridge, Mass.: Project MAC, MIT, September 1970.

25. L.G. Roberts, "Machine Perception of Three-Dimensional Solids," Lincoln Laboratory Technical Report 315,22. Lexington, Mass., May 1965.

26. J.G. Advani, "Computer Recognition of Three-Dimensional Objects from Optical Images," Ph.D. Dissertation, The Ohio State University, August 1971.

27. R.L. Pio, "Euler Angle Transformations," IEEE Transactions on Automatic Control, Vol. AC-11, No. 4, October 1966.

28. R.L. Pio, "Symbolic Representation of Coordinate Transformation," IEEE Trans. on Aerospace and Navigational Electronics, Vol. ANE-11, pp. 128-134, June 1964.

29. T.M. Cover, "Nearest Neighbor Pattern Classification," IEEE Trans. on Information Theory, Vol. IT-13, No. 1, January 1967.